Chem Soc Rev

Polyether Complexes of Groups 13 and 14

Journal:	*Chemical Society Reviews*
Manuscript ID	CS-REV-12-2015-000934.R1
Article Type:	Review Article
Date Submitted by the Author:	29-Mar-2016
Complete List of Authors:	Swidan, Ala'aeddeen; University of Windsor, Department of Chemistry and Biochemistry Macdonald, Charles; University of Windsor, Department of Chemistry and Biochemistry

Polyether Complexes of Groups 13 and 14

Ala'aeddeen Swidan and Charles L. B. Macdonald*

Department of Chemistry and Biochemistry, University of Windsor, 401 Sunset Ave. Windsor, ON, N9B 3P4, Canada

Phone: 1-519-253-3000 ext.3991

Email: cmacd@uwindsor.ca

Abstract

Notable aspects of the chemistry of complexes of polyether ligands including crown ethers, cryptands, glycols, glymes, and related polyether ligands with heavier group 13 and 14 elements are reviewed with a focus on results from 2005 to the present. The majority of reported polyether complexes contain lead(II) and thallium(I) but recent breakthroughs in regard to the preparation of low oxidation state reagents of the lighter congeners have allowed for the generation of complexes containing indium(I), gallium(I), germanium(II), and even silicon(II). The important roles of ligand size, donor types, and counter anions in regard to the chemical properties of the polyether complexes is highlighted. A particular focus on the structural aspects of the numerous coordination complexes provides a rationale for some of the spectacular contributions that such compounds have made to *Modern Main Group Chemistry*.

Keywords

Crown ethers, polyethers, cryptands, podands, group 13, group 14, triel, tetrel, low oxidation state, low valent, coordination chemistry

1. Introduction

Since their discovery,[1, 2] crown ethers and related polyether ligands have been employed as ligands for a variety of substrates. The binding ability of such molecules was first exploited to bind metal ions – particularly those from the s-block[3] – sometimes with spectacular results such as electride salts.[4] The properties of polyether donors have since been used to prepare complexes of small molecules[5] and even to generate supramolecular assemblies[6]. Numerous applications associated with the binding and ligand chemistry of polyethers have been developed over the last 50 years and range from ion sensing,[7-9] separation[10] and binding, to supramolecular chemistry[11] and molecular machines, to synthetic ion channels[12] and biomedical applications,[13-15] permanently porous liquids,[16] and much more.

Because of the breadth of the topic and the extensive coverage of the chemistry of crown ethers and related ligands in books and reviews, the work that will be presented in the present *Modern Main Group Chemistry* "themed" review is not intended to be exhaustive but has been selected by the authors to be representative of important developments in the general area of low valent p-block chemistry. In particular, we examine compounds featuring elements from groups 13 ("triels") and 14 ("tetrels") in relatively low oxidation states bound by polyether ligands featuring at least three donor sites and least one vicinal diether fragment. This review will largely feature work reported since 2005 but selected older examples are presented where appropriate. Finally, given that structural characterization is often necessary to authenticate the nature of the complexes and their geometrical features, the classes of compounds treated in this review are largely restricted to those that have been characterized by single crystal X-ray diffraction (scXRD) and are reported in the Cambridge Structural Database (CSD; the CSD codes for important examples are included to assist further investigations by interested readers).[17] All of the molecular structure drawings in this work were made using the XP

application in the SHELXTL[18] package and, for disordered structures, only the form with the highest occupancy is depicted.

In order to facilitate the description of the complexes presented in this review, it is worth defining the nomenclature convention we employ. Rather than using formal IUPAC nomenclature, we use a nomenclature system that is commonly used by researchers in the area. In general, crown ethers are labeled using the template: **[m]crown-n**, in which **m** indicates the total number of atoms in the heterocycle and **n** indicates the number of O atoms. A prefix may precede the brackets in order to indicate the replacement of an ethylene bridge by another functionality; typical examples are: B = benzo, C = cyclohexyl, DB = dibenzo, DC = dicyclohexyl. Thus, the original crown ether **A** in Scheme 1 would be designated **DB[18]crown-6**. The related saturated polyether ligands in which oxygen atoms have been formally replaced by other donor atoms are named **[m]ane-O_iE_j**, in which E is the other donor atom (e.g. S, Se, NR, PR, etc.) and the subscripts i and j specify the number of each type of donor. Thus the ligand **B** in Scheme 1 would be designated **[18]ane-O_4S_2**. Unsaturated analogues of such ligands may be specified using the general form **[m]ene-O_iE_j**, etc. The final major class of ligands covered in this review are the cryptands, which are named using the form **crypt[x,y,z]**, in which **x**, **y**, and **z** are integers that indicate the number of O atoms in each bridging arm of the ligand. Thus the most commonly used cryptand ligand, **C** in Scheme 1, is called **crypt[2.2.2]**. Line drawings will be presented for polyether ligands that are too complex to be named using the simple convention described above.

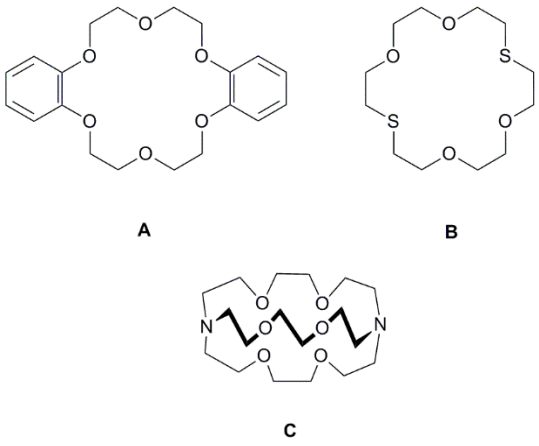

Scheme 1. Crown ether nomenclature examples. **A**: DB[18]crown-6, **B**: [18]ane-O_4S_2 and **C**: crypt[2.2.2].

Although this review will demonstrate that p-block elements from groups 13 and 14 may be bound in a variety of manners by the polyether ligands, perhaps one the earliest recognized and typical features of crown ether ligands is their ability to encapsulate ions of appropriate size in a belt-like (*meridional*) manner to provide Saturn-like complexes. The estimated cavity diameters of the most common crown ether ligands used to bind the p-block elements in Scheme 2A and the estimated ionic radii of group 13 and 14 ions are presented in Table 1. Please note that the ranges of cavity sizes that have been established for crown ethers[19] – generally on the basis of studies with well-defined s-block metal ions – can be used to estimate the size of some of the more unusual p-block ions described herein but such estimates must always be treated with some skepticism because of the inherent flexibility of the heterocyclic ligands. Furthermore, if a metal ion is too large to be bound in a *mer*-like manner by a particular polyether, it is still possible for complexation to occur to generate "sunrise" or "half-sandwich", or *facial*- complexes with a single ligand, or "sandwich" complexes with two ligands, etc. (Scheme 2B)

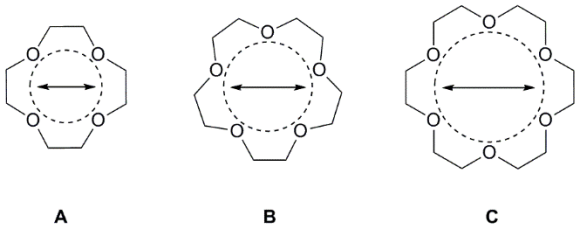

Scheme 2A. Ranges in crown ether cavity sizes expressed in terms of the apparent internal diameter (d)[19] and ligand cavity radius (r)[20]. **A**: [12]crown-4, d: 1.2-1.5 Å, r: 0.60 Å; **B**: [15]crown-5, d: 1.7-2.2 Å , r: 0.85 Å; **C**: [18]crown-6, d: 2.6-3.2 Å, r: 1.30 Å.

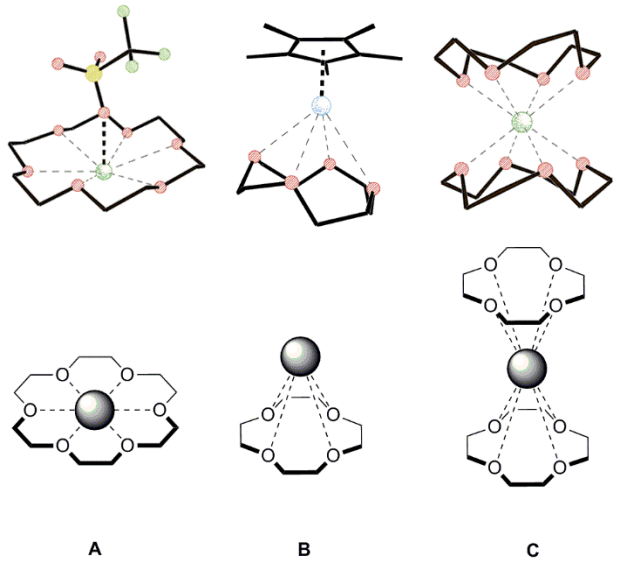

Scheme 2B. Examples showing typical modes of complexation of a metal ion to a crown ether. **A**: when the metal ion is located completely within the ligand cavity (*meridional-like*, *mer*-) – the typical interpretation is that the radius of the metal ion is smaller than that of the ligand cavity; **B**: when the metal ion is not located within the cavity of the ligand such that only a portion of one hemisphere of the coordination environment is bound by the ligand (*facial-like, fac*-) – the typical interpretation is that the radius of the metal ion is larger than that of the ligand cavity; **C**: when the metal ion is bound in a *fac*-like manner by two ligands (sandwich).

Table 1. Shannon-Prewitt (S-P)[a] ionic radii (6-coordinate "crystal" radii) [21] and Alvarez covalent radii[22] (in Å) for group 13 and 14 cations and atoms and selected anions

Group 13	S-P	Covalent	Group 14	S-P	Covalent
Al^{3+}	0.675	1.21	Si^{4+}	0.54	1.11
Al^{1+}			Si^{2+}		
Ga^{3+}	0.76	1.22	Ge^{4+}	0.67	1.20
Ga^{1+}			Ge^{2+}	0.87	
In^{3+}	0.94	1.42	Sn^{4+}	0.83	1.39
In^{1+}			Sn^{2+}	1.22	
Tl^{3+}	1.025	1.45	Pb^{4+}	0.915	1.46
TlI^{1+}	1.64		Pb^{2+}	1.33	
Group 16	S-P	Covalent	Group 17	S-P	Covalent
O^{2-}	1.26	0.66	F^{-}	1.19	0.57
S^{2-}	1.70	1.05	Cl^{-}	1.67	1.02
Se^{2-}	1.84	1.20	Br^{-}	1.82	1.20
Te^{2-}	2.07	1.38	I^{-}	2.06	1.39

[a] Please note that S-P cationic "crystal" radii are always larger than Pauling's ionic radii because S-P radii define the radius of O^{2-} as 1.26 Å whereas Pauling's scale defines the radius for O^{2-} as 1.40 Å.

Given the incredibly propensity for crown ethers and related ligands to bind ions of the unambiguously metallic s-block elements, it is perhaps not surprising that the vast majority of complexes of p-block contain the element in a relatively low oxidation state. By definition, elements in

lower oxidation states are more electron-rich and thus less electronegative than their higher oxidation state congeners.[23, 24] For the elements at the left-hand side of the p-block, an ion in a lower oxidation state will behave more like that of an s-block metal (e.g. featuring lower ionization energies, electron affinities, and charge densities) and render it more likely to engage in the coordinative and primarily electrostatic (ion-dipole) interactions that characterize the binding with the polyether complexes. Periodic trends favor lower oxidation states within a group as the atomic number increases so there are usually considerably more polyether complexes of the heavier elements within a group. In fact, the prevalence of such complexes for the heaviest group 13 and 14 elements has allowed for the thorough investigation of solution properties (including, for example, the determination of stability constants of crown ether complexes in a variety of solvents) only for Tl^{+}, Pb^{2+} and Sn^{2+} ions.[20] It should be noted that the presence of non-bonding electrons in low valent p-block atoms renders them softer than the comparable s-block analogues, which may affect the nature of the binding in certain instances – particularly for polyethers that contain heavier group 16 donor sites. At this point, it is also worth reminding the reader that oxidation state and valence state are not synonymous[25] but the primarily non-covalent nature of the binding in complexes of ligands such as crown ethers often results in coincidental assignments. For example, the indium atom in the complex [In([18]crown-6)][O_3SCF_3][26] is *univalent* and has an oxidation state of +1 but such agreement is neither general nor necessary. In contrast, the pseudo-dicoordinate indium atom (in bold-face) in the complex [**In**Cl([18]crown-6)–$InCl_3$][26] (UWAVEU) is most accurately described as *trivalent* and the formal oxidation state may be +1 or +2 depending on the manner in which the electrons are counted and partitioned.[27]

As indicated above, there have been numerous reviews of the chemistry of crown ethers and related ligands so we aim to use this review to illustrate complexes that we find instructive in the context of the modern area of low valent, p-block main group chemistry. The material is divided in terms of periodic table group, starting with the heavier elements for the reason described above. As

also noted above, the most definitive characterization of polyether complexes of group 13 and 14 elements in the solid state has typically been accomplished using crystallography. Of course, other means of characterization – particularly for solution chemistry – have been used, including: multinuclear NMR spectroscopy, mass spectrometry, UV-vis and fluorescence spectroscopy, electrochemistry, and other methods. The results from many experiments using these methods demonstrate that such polyether complexes exhibit dynamic and fluxional behavior in solution that sometimes renders the interpretation of the results non-trivial. For example, the changes in ^{1}H NMR signals for the methylene protons in crown ethers between the free ligand and the metal complexed form are often less than 0.05 ppm;[28] for symmetrical crown ethers in particular, such subtle changes in the spectra – coupled with the fluxional nature of such complexes – often limits the diagnostic utility of the technique. Similarly, whereas certain mass spectrometric techniques can provide information regarding the composition of ions present, most do not offer unambiguous information regarding how a complex is bound by the ligand. In this light, we have chosen to focus our coverage on classes of complexes that have been structurally authenticated and we provide relevant data for the associated solution chemistry. In general, we have selected representative work to be described in detail for classes of related complexes (e.g. when different counter-anions do not appear to alter the behavior of a given cation) but the total number of CSD hits for each element is noted in order to illustrate the relative number of compounds that have been characterized by crystallography.

2. Group 14

The periodic trends in group 14 [29] result in lead(II) being the most common and stable of the tetrel(II) ions. As a result, the vast majority of known polyether complexes of the tetrel group contain that ion (114 of a total of 185 CSD reports for group 14). The relative favorability of tin(II) also allows for a significant number of known complexes (55 reports in the CSD). In contrast, the development of polyether complexes of germanium and silicon – for which the divalent forms tend to be air- and moisture-sensitive – is a much more recent development and there are much fewer examples reported: there are 15 reports in the CSD for Ge and only a single example for Si.

2.1 Lead

The historic use of lead plumbing, solder, paint, and gasoline additives – in conjunction with the well-established toxicity of the element – prompted extensive research into the identification and selective removal of the element; most of the early research into the complexation of lead with polyethers and related ligands may be understood in that very general context.[30] More recently, the tremendous interest in perovskite materials containing lead halides, primarily for potential photovoltaic applications,[31] has resulted in many new fundamental investigations, including some that involve polyether ligands.

2.1.1 Lead(II)

Early attempts to stabilize Pb(II) with different crown ethers were performed by groups including those of Rogers[32, 33], Murphy and Fenton[34] and Fenske[35]. The work by Murphy and Fenton involved a macrocyclic ligand containing an N_3O_3 donor set (Figure 1). In early attempts to bind Pb^{2+}, much of the work employed nitrogen-containing macrocycles due to the better match of the softer N

donor with the soft Pb^{2+} cation.[32] Much more recent work with related ligands demonstrates the plausibility of this idea; in the lead(II) complex of a related Schiff-base polyether hybrid ligand (FOPJOK, Figure 1), the Pb^{2+} ion appears to interact exclusively with the nitrogen portion of the molecule rather than with the polyether fragment.[36] However, even by the late 1980's , Hancock had suggested that the use of nitrogen donors in a macrocycle may result in an increased stereochemical activity of the lone pair which could introduce another variable into the complexation chemistry and potentially affect the separation of Pb^{2+}.[37] Thus, for the past two decades, a large number of stable complexes of lead(II) have featured poly(ethylene glycol) (PEG) based crown ethers and analogous acyclic polyether ligands.[33]

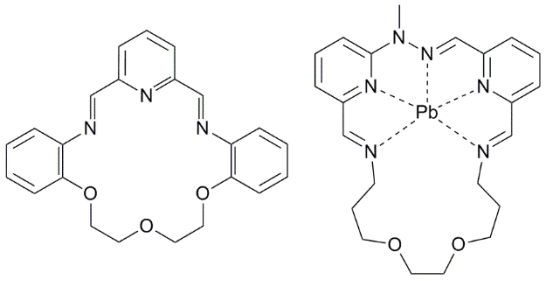

Figure 1. Left: N_3O_3 ligand system employed by Murphy and Fenton; Right: FOPJOK, the structure is authenticated with scXRD, but a chemical drawing is presented for clarity.

For example, Rogers and co-workers found that the reaction of $Pb[NO_3]_2$ with any of several common crown ethers and acyclic polyethers can be used to produce crystalline crown ether complexes. Many of these were structurally characterized and an example of one, the pentaethylene glycol (EO5) complex $[Pb(EO5)][(NO_3)_2]$ (RABKEK) is shown in Figure 2.[32, 33] This complex illustrates how an unconstrained polyether can bind to lead(II) in a *mer*-like manner and features Pb···O distances ranging from 2.650(5) – 2.847(5) Å.

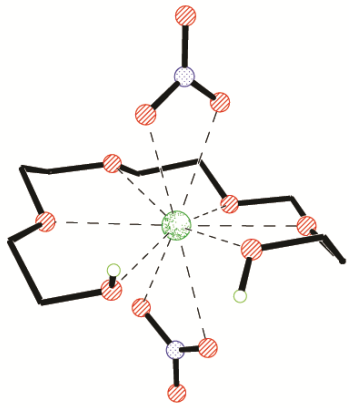

Figure 2. [Pb(EO5)][$(NO_3)_2$]– RABKEK

Among the numerous interesting compounds reported by Rogers is one containing $[PbBr(EO5)]^+$ cations arranged about a polymeric $[PbBr_3]^-_n$ anionic structure that propagates along one of the unit cell axes. The material was prepared by stirring $PbBr_2$ with the appropriate polyethylene glycol (EO4, EO5, EO6 and EO7) at 60°C for an hour to result in structures featuring such polymeric anions (RABKOU, RABKUA and RABLAH). Each of these materials also feature cations of the general form $[PbBr(EOx)]^+$ (x = 5, 6, 7) but the EO6 material has the overall formula $[PbBr(EO6)]_2[PbBr_2(EO6)][PbBr_3]_2$ and contains an additional neutral PEG complex of the type $PbBr_2$(EO6), which features a linear Br-Pb-Br unit. In work that is conceptually related, Chekhlov and co-workers reported numerous polyether complexes of lead(II) including many that were structurally characterized.[38-44] Of particular relevance is the crown ether salt [PbBr[18]crown-6][$PbBr_3$] (Figure 3, COTXIT) in which the crystal structure contains infinite chains of $[PbBr_3]^-_n$ anions oriented along one of the unit cell axes. [38] In this instance, two of the bridging bromide anions act as a common edge to this polymeric chain as shown in the figure. In all of the materials described above, the lead(II) ions in the polymeric anionic component exist in roughly octahedral environments and are thus reminiscent of the anionic structures found in group 14 halide perovskites with the general form [cation][MX_3] ($M = Sn^{II}, Pb^{II}$; X = Br, I).[31] In a more general context, the incredible potential for the use of group 14 halide perovskites for photovoltaic applications has resulted

in a vast amount of interest[45] in the last 5 years and has even received attention in non-scientific media.[46]

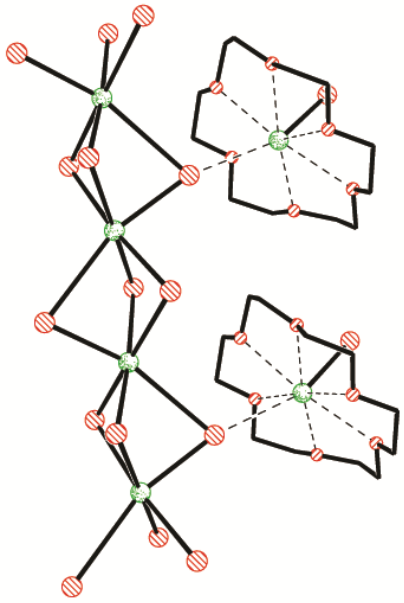

Figure 3. $[Pb_2Br(\mu_2\text{-}Br)_2(\mu_3\text{-}Br)([18]crown\text{-}6)]_n$ – COTXIT

Interestingly, most ferroelectric materials[47, 48] used for electronic applications also come from a perovskite family of inorganic ceramics.[49] Ferroelectric materials are capable of undergoing phase transition which allows for a spontaneous polarization that can be directed by an applied field. This property allows for numerous applications such as capacitors, ultrasound imaging, data storage, switches, oscillators and many others.[39] The typical methods employed to prepare such perovskites (e.g. $BaTiO_3$) require high temperatures that are unsuitable for many desirable substrates thus molecular-based alternatives are desirable. Reid and co-workers have reported the preparation and structure of the complex $[Pb[15]crown\text{-}5][NO_3]_2$ (Figure 4, FIBZOH);[49] Xiong and co-workers synthesized the same compound and other analogous complexes with different metal centers (Ca^{2+}, Cd^{2+}, Pb^{2+} and Co^{2+}).[48] Investigations of the dielectric properties of $[Pb[15]crown\text{-}5][NO_3]_2$ showed evidence for a ferroelectric transition, illustrating the potential of such easily synthesized and relatively simple materials.

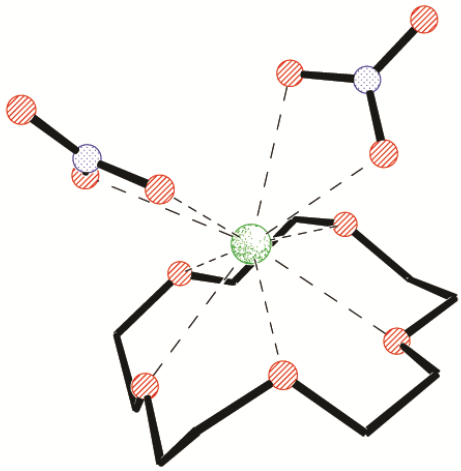

Figure 4. [Pb([15]crown-5)][$(NO_3)_2$] – FIBZOH

It should be noted that Reid and co-workers had prepared [Pb[15]crown-5][$NO_3]_2$ as part of an extensive investigation of the structural features of lead(II) crown ether complexes.[49] This study included the preparation and structural characterization of complexes of lead(II) with crown ethers and related ligands including: [18]crown-6, [15]crown-5, [15]ane-O_3S_2, [18]ane-O_4S_2, and [18]ane-O_4Se_2, and featuring counter ions including $[BF_4]^-$, $[NO_3]^-$, and $[PF_6]^-$ (see, e.g.: FIBZAT, FIBZOH, FIBZIB, FIBYOG, FIBYUM, FIBZEX, FIBZIB, REPHIF, RERVIV, RERVOB). In several instances, the materials were also prepared using aqueous solutions. The observations from the structural data allowed the authors to conclude that, although there are dramatic differences in the geometrical features observed, it does not appear as if there is evidence for the presence of a stereochemically-active non-bonding pair of electrons on any of the lead(II) ions! In fact, it appears as if the large Pb^{2+} ion will readily interact with any available donors in order to fill its coordination environment and that the overall coordination number observed (usually 8-11) is subject only to the constraints of the donor groups. Spectroscopic studies suggest that the complexes exhibit fluxional behavior in solution that prevents the observation of a signal in the ^{207}Pb NMR spectrum – such behavior is not uncommon for polyether complexes of lead(II) (and tin(II)) and often precludes meaningful NMR investigations or even the acquisition of usable

spectra – and the authors concluded that the data suggest that the potential energy well for the binding of lead(II) is very shallow such that many of the peculiar features observed in the solid state are attributable to packing interactions.

The ability of polyether ligands to occupy numerous sites in the coordination environment about lead has also been used in practical applications. For example, lead-containing films remain materials of interest for many industrial applications.[50] Chistyakov[51-53] and co-workers employed the complex [Pb[18]crown-6][NO_3]$_2$ (JUCCEP02) as reagent with either NH_4(hfa) or NH_4(tfa) (hfa = hexafluoroacetylacetonate; tfa = trifluoroacetylacetonate) to produce the compounds [Pb[18]crown-6][hfa]$_2$ (MIFSIE) and [Pb_2[18]crown-6][tfa]$_4$ (VOHLAG) (Figure 5), respectively. These materials were prepared and investigated as coordinatively saturated chemical vapor deposition (CVD) precursors for lead oxides.

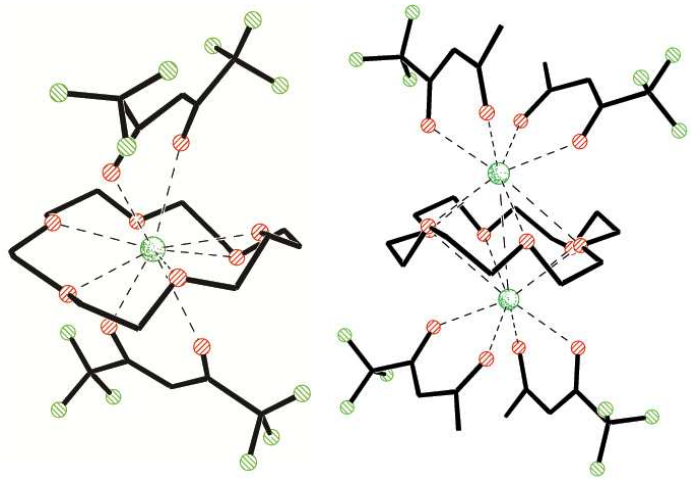

Figure 5. [Pb[18]crown-6][Hfa]$_2$ (Left, MIFSIE) and [Pb_2[18]crown-6][Tfa]$_4$ (Right, VOHLAG).

In a similar vein, Fragalà and co-workers reported the direct synthesis of a polyether adduct of a lead(II) hexafluoroacetylacetonate complex ([Pb(hfa)$_2$·diglyme]$_2$) (Scheme 3) that proves to be an excellent precursor for the preparation of lead-containing films (particularly PbO) by Metal Organic Chemical Vapor Deposition (MOCVD).[50, 54] MOCVD is one of many deposition techniques but the great

precision with which layers of a material can be grown using this approach renders it particularly applicable for optoelectronic applications. Moreover, MOCVD is one of the most convenient deposition processes for scale up to an industrial scale.[50] In general, MOCVD processes require highly volatile and thermally stable materials that will decompose cleanly on a substrate surface; any premature decomposition will lead to species with low volatility.[55] Although $[Pb(hfa)_2 \cdot diglyme]_2$ (Figure 6, ABUTEX) is dimeric in nature,[50, 56] the ligation by the polyether provides a molecular material in contrast to free $Pb[hfa]_2$, which adopts an infinite coordination polymeric structure.[57] Consequently, thermal analyses of $[Pb(hfa)_2(diglyme)]_2$ revealed high volatility and sufficient thermal stability for it to be used successfully as a unique liquid-phase precursor to PbO films.

$$2PbO + 4Hhfa + 2diglyme \rightarrow [Pb(hfa)(diglyme)]_2 + 2H_2O$$

Scheme 3. Reaction scheme showing the synthesis of the lead(II) hexafluoroacetylacetonate polyether complex MOCVD precursor.

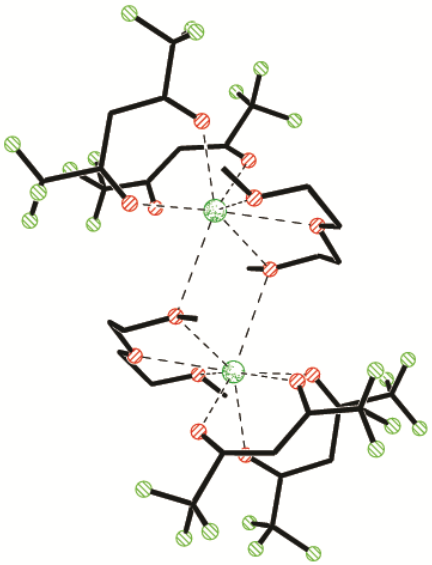

Figure 6. $[Pb(hfa)_2(diglyme)]_2$ – ABUTEX

Interest in metal-organic frameworks (MOFs) has grown tremendously over the past two decades.[58] The investigation of MOFs has revealed how metal-ion coordination chemistry and ligand design can lead to materials with unusual structures and properties, [59] which have proven to be useful in gas storage and many other applications.[60] In an effort to synthesize an organic-inorganic hybrid framework featuring crown ethers, Dou and co-workers[61] synthesized a polymeric complex $[[Pb(DC[18]crown\text{-}6)(H_2O)][Pd(SCN)_4]]_n$ (DC[18]crown-6 = cis-syn-cis-dicyclohexyl-[18]crown-6) (Figure 7, GAVDOX). The material was prepared by the reaction of DC[18]crown-6 with $PdCl_2$ and $Pb[SCN]_2$. The $[SCN]^-$ groups on the palladium anion link with adjacent lead(II) complexes to form a coordination polymeric chain. Dou and co-workers later reported an analogous coordination polymer (IDAXER) featuring [18]crown-6 in lieu of DC[18]crown-6.[62]

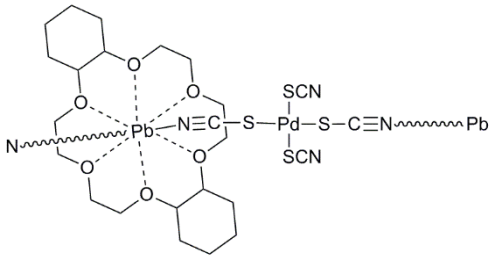

Figure 7. $[Pb(DC[18]crown\text{-}6)(H_2O)][Pd(SCN)_4]$ – GAVDOX

Among the novel examples of Pb(II) crown ether complexes that were reported by Feldmann and co-workers[63] is the interesting lead(II) stannate salt $[Pb_2I_3([18]crown\text{-}6)_2][SnI_5]$ (Figure 8, LADKEI), which was prepared by the reaction of PbI_2, SnI_4 and [18]crown-6 in the ionic liquid $[NMe(^nBu)_3][N(OTf)_2]$. The explicit use of the ionic liquid was to provide the reaction with a polar but aprotic environment which would allow for the fast diffusion of the reactants at a relatively moderate temperature (≤ 100 °C). The geometry about the bridging iodide atom in the cationic fragment of the complex is bent, while the tin center adopts a conventional trigonal-bipyramid geometry. As one would anticipate, the Pb–I bonds to the terminal iodide atoms are significantly shorter (2.927 Å) than are those

to the bridging iodide (3.504 Å) so the complex may be reasonably interpreted as [(PbI([18]crown-6))$_2$(μ^2-I)][SnI_5].

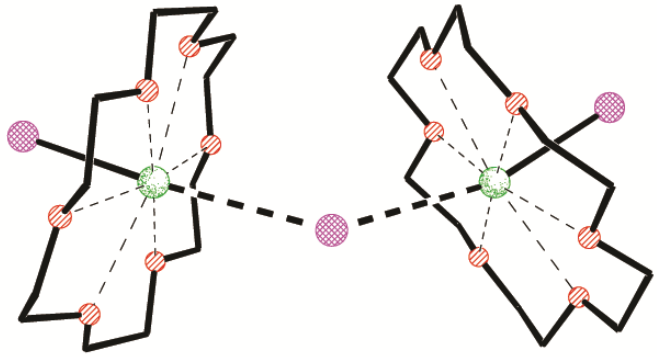

Figure 8. $[Pb_2I_3([18]crown\text{-}6)_2]^+$ – LADKEI

Interestingly, and in contrast to the ionic complexes described above, Reiger and Mudring found that the coordination of $PbCl_2$ with [18]crown-6 actually results in a "molecular" complex with the composition $PbCl_2$[18]crown-6 (denoted as $PbCl_2$@[18]crown-6 in that work) (Figure 9, NOMJUV).[64] In the solid state, the complex exhibits D_{3d} symmetry with Pb-Cl bonds of 2.765(2) Å and Pb···O distances of 2.751(2) Å. The absence of evidence for a stereochemically active pair of non-bonding electrons was noted and is consistent with the conclusions of Reid described above.

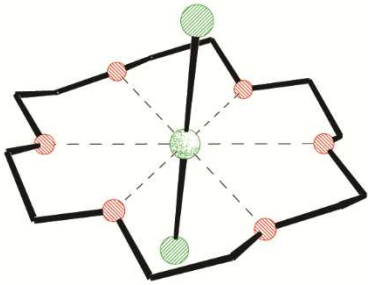

Figure 9. $PbCl_2$[18]crown-6 – NOMJUV

The structural aspects of mixed-donor macrocyclic compounds have been extensively reviewed over the past few decades.[65, 66] As indicated above, Reid and co-workers recently reported multiple lead(II) crown ether complexes that include Se/O and S/O mixed macrocycles.[49] Treating lead tetrafluoroborate with one equivalent of [18]ane-$O_4S_2(H_2O)_2$[results in colorless crystals [Pb([18]ane-O_4S_2)$(H_2O)_2$[BF_4]][BF_4] (Figure 10, FIBZEX). The analogous reaction employing the smaller [15]ane-O_3S_2 macrocycle (2:1 crown to Pb) results in [Pb([15]ane-O_3S_2)]$_2$[BF_4]$_2$ (Figure 11, FIBZAT), which features a distinct sandwich dicationic component. Although the lead(II) center can be considered as 10-coordinate, two of the Pb–O distances are substantially longer than the other Pb–O bonds (2.898(5) and 3.055(5) Å versus the range of 2.688(5)-2.750(4) Å for the other Pb–O bonds) which might make it more appropriate to be considered an 8-coordinate core. Lee and co-workers reported similar mixed-donor macrocyclic compounds in which the same macrocycle is used but with different lead sources to end up with two compounds that are geometrically different.[65] Treating the macrocyclic ligand [18]ane-O_4S_2 with Pb[ClO_4]$_2$ or with Pb[NO_3]$_2$ in benzonitrile resulted in compounds **1** and **2** respectively as shown in Scheme 4. Compound **1** is 6-coordinate (distorted octahedral) with a *trans* arrangement of the perchlorate anions and features long contacts between the sulfur atoms and the lead(II) center (Pb–S, 3.0906 (8) Å). Conversely, compound **2** features a macrocycle with a boat-like conformation and the two nitrate ions each bind as bidentate ligands on a single face to the metal opposite the bound macrocycle. The Pb···O distances to the oxygen atoms of the polyether in the perchlorate salt are slightly longer than are those in the nitrate salt which was interpreted in terms of a stronger interaction of the anions in **1** (compared to **2**) resulting in an 8-coordinate complex.[65] However, as suggested by Reid, the shallow potential for the binding of polyethers with lead(II) often results in conformations that are attributable to packing forces so the differences observed may not be attributable exclusively to anion-lead interactions.

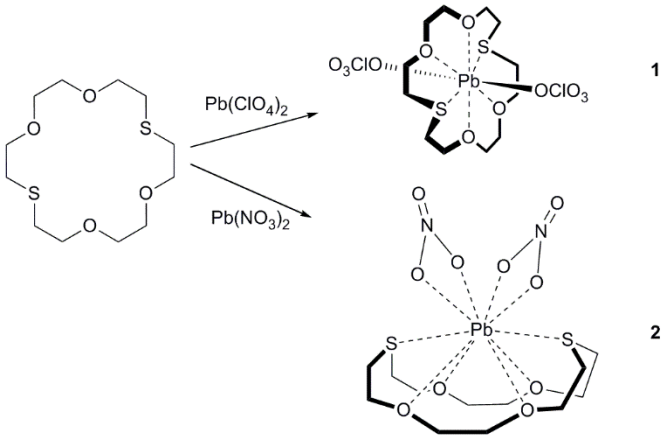

Scheme 4. Reaction scheme showing the different products obtained from the different Pb(II) starting materials.

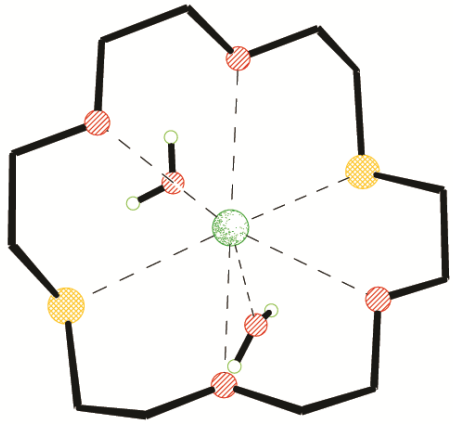

Figure 10. $[Pb([18]aneO_4S_2)(H_2O)_2]^{2+}$ – FIBZEX

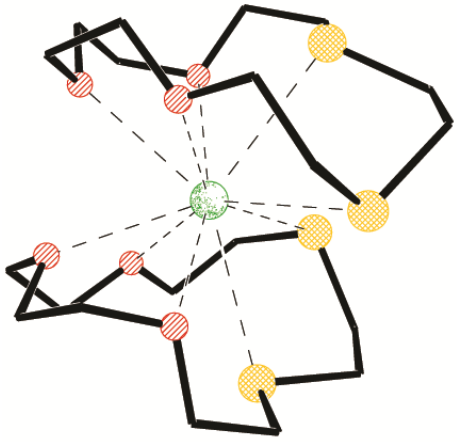

Figure 11. $[Pb([15]aneO_3S_2)_2]^{2+}$ – FIBZAT

Because of the well-known environmental and health concerns about lead, authorities have already restricted many uses of lead in order to the decrease the levels of lead in the environment.[67] Furthermore, removal of heavy metal contaminants from water remains an important environmental concern that has resulted in extensive investigation.[68] In the context of polyether chemistry, de Blas and co-workers synthesized a hybrid Schiff-base polyether macrobicycle (L^4 in the scheme below). They found that refluxing the salt $[Ba(L^4)][ClO_4]_2$ with $Pb[ClO_4]_2{\cdot}6H_2O$ in absolute ethanol yielded a yellow precipitate characterized as $[Pb(L^4)][ClO_4]_2{\cdot}0.5H_2O$, (Figure 12, HIFHAG).[68] The results of further investigations by that research group were used to provide a rationale for the various conformations adopted by the different Schiff-base macrobicycles about the lead(II) centers.[68-76] Overall, the authors found that the large cavity of their ligand system allows for much structural variation that is dependent on the nature of the counter anions associated with lead(II) ions and the pH of the system. Importantly, they discovered that treatment of the lead(II) complex of a pyridinyl-derived macrocyclic ligand (e.g. RARZOA) with acid allows for the decomplexation of the encapsulated lead ion; such behavior suggested that such ligands may be suitable for remediation applications.

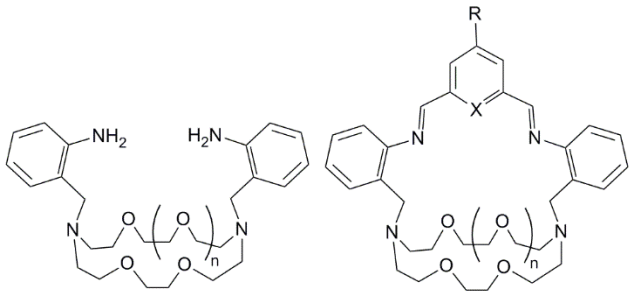

L^1: n = 1
L^2: n = 2

L^3: n = 0, R = H, X = N
L^4: n = 0, R = CH_3, X = C-OH
L^5: n = 1, R = H, X = N
L^6: n = 1, R = CH_3, X = C-OH

Scheme 5. Different Schiff-base macrobicycles and their abbreviations.

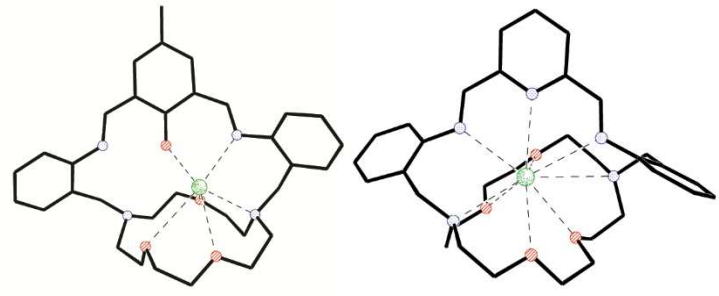

Figure 12. Top: Schiff-base macrobicycle ligands; Left: $[Pb(L^4)]^{2+}$– HIFHAG; Right: $[Pb(L^5)]^{2+}$ – RARZOA

Dyes of the type illustrated in Figure 13 containing crown ether fragments were found to undergo a change in the long-wavelength absorption band upon binding to a metal cation.[77] The change in absorption – which are much greater than, for example, changes in NMR spectra – renders such compounds potentially useful for different applications including the detectable phase transfer of salts and the study of ion transport.[78] Another potential application of such macrocycles that has been proposed is the development of optical molecular sensors suitable for the detection of transition and heavy metal cations.[77] In this context, Gromov and co-workers synthesized dithiacrown-containing butadienyl dyes (Figure 13, ligands **3** and **4**) in order to investigate the binding of such dyes with different heavy metal cations.[77] They found that the treatment of such crown ether dyes with $Pb(ClO_4)_2 \cdot 3H_2O$, resulted in the formation of complexes of the type illustrated in Figure 14 (KAMGUC). The authors noted that the conformation of the free macrocycle is relatively flat, but upon binding to Pb^{2+}, the conformation of the macrocycle adopts a crown-like conformation. As anticipated, different heavy metals exhibit different binding affinities to these dyes; in the case of macrocycle **4b**, the stability constants in acetonitrile showed a change in the following sequence: $Cd^{2+} < Ag^{+} < Pb^{2+} << Hg^{2+}$.[77]

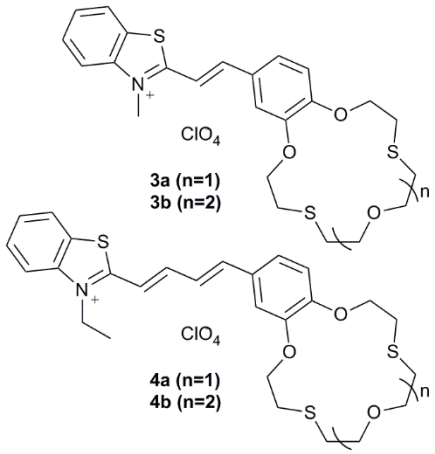

Figure 13. Dye-containing crown ligands **3** and **4**.

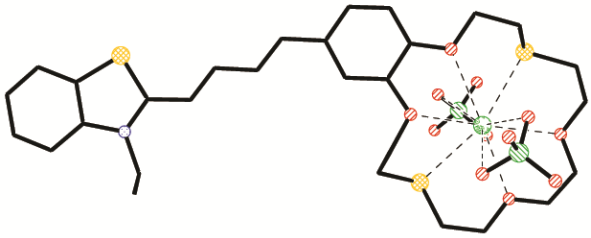

Figure 14. [Pb·**4b**][ClO_4]$_2$ – KAMGUC

Photo-induced electron transfer (PET) is currently the most extensively used method for sensing metal ions in solution.[79] The typical design of PET sensors is based on the concept that, upon complexation of a metal ion, electron transfer within the receptor guest is interrupted and luminescence is switched on. Sykes and co-workers reported an alternative method for sensing metal ions in solution using a hybrid polyether anthraquinone ligand. The authors selected this molecule in order to exploit the low-lying n-π* transition in this system. Although the n-π* transitions in this compound generally do not luminesce, the binding an electropositive center raises the energy of the n-π* transition above that of the π–π* transition and allows luminescence to occur.[80, 81] The researchers illustrated that the use of compound **5** (Figure 15) can function as such a turn-on sensor. For example, the treatment of **5** with one equivalent of lead perchlorate in acetonitrile leads to a 1:1 metal/ligand complex [Pb(**5**)][ClO_4]$_2$

with the structure shown in Figure 16 (PECQAQ). The photophysical properties of several other metal complexes were investigated in detail. The absorbance spectra of the system exhibit significant changes upon titration of **5** with lead perchlorate (0.2 increments of $Pb[ClO_4]_2$) and isosbestic point is observed upon adding one equivalent of Pb^{2+}, which is consistent with the formation of the 1:1 metal/ligand complex.[81, 82] Perhaps the most notable structural feature of the system is that the endocyclic carbonyl oxygen is greatly bent out of the anthraquinone plane which also results in the anthraquinone becoming non-planar (the dihedral angle between the two aromatic rings in anthraquinone is ~20°). These structural changes appear to be key to changes in luminescence: the zinc analog of this complex, which features a dihedral angle of ~2°, is not luminescent, whereas both the calcium(II) and lead(II) complexes – each of which features a dihedral angle of ~20° – are luminescent. The authors noted that many interactions, including those with anions and with solvent affect the performance of such sensors.

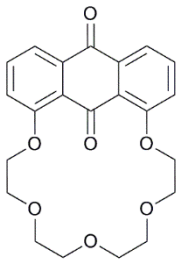

Figure 15. Compound **5**.

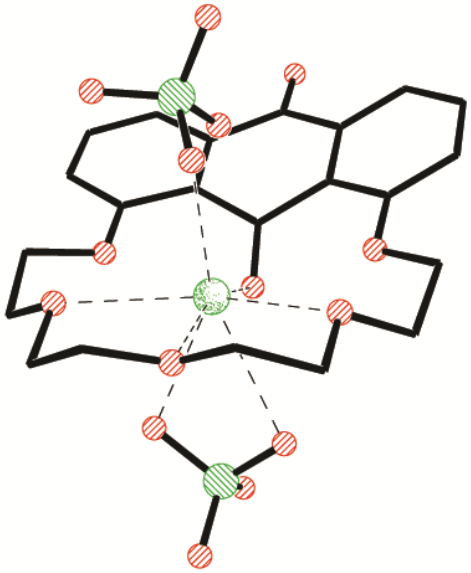

Figure 16. [Pb-**5**][ClO_4]$_2$ – PECQAQ

Further related chemosensor investigations by Kim and co-workers also featured sensor ligands containing the 9,10-anthraquinone functionality and illustrates the importance of ligand design.[83] They discovered that the treatment of the hybrid calixaene-crown-9,10-anthraquinone derivative (**6**) with Pb[ClO_4]$_2$ resulted in compound [Pb(**6**)(H_2O)($MeCN$)$_3$][ClO_4]$_2$ (Figure 17, POZCUD). The crystal structure of the complex reveals that the Pb^{2+} is coordinated to the crown-6 portion of the molecule and not the crown-anthraquinone cavity. This mode of coordination does not result in a change in absorption in UV-vis upon coordination of a Pb^{2+} ion and thus limits it use as a sensor for lead(II).[83]

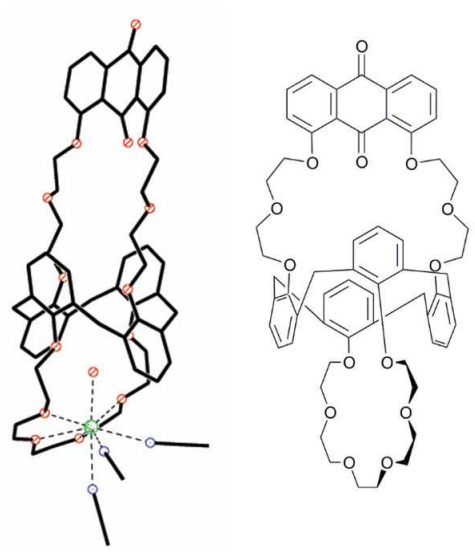

Figure 17. Left: $[Pb(\mathbf{6})(H_2O)(MeCN)_3][ClO_4]_2$ – POZCUD; hydrogen atom positions for the water were not in the CSD record. Right: Ligand **6** (1,3-alternate calix[4]crown-6 anthraquinone).

As illustrated by the numerous examples above, the specific nature of the binding of a macrocycle to lead(II) (and other target ions) can have a dramatic effect on the properties of the resultant complexes. Ideally, such fine-tuning of the donor arrangement within the macrocyclic ligand structure could offer some control over the coordination mode and connectivity of their metal complexes but the importance of counter-ion interactions, and solvent interactions and even the properties of metal center itself cannot be discounted.[84] Although macrocycles composed of polyethers often induce endocyclic coordination, the incorporation of thioether units as donor sites within the crown, often results in exocyclic coordination because of the tendency of sulfur to orient itself in an manner that favors such coordination.[85] It should be emphasized that exocyclic complexes are attractive because of the possibility of their use in the formation of coordination polymer networks. While such endocyclic coordination is certainly observed for many poly(thio)ether complexes (i.e. featuring **[m]ane-S_i** ligands),[65, 66] as demonstrated above, the inclusion of only a few thioether units into a flexible polyether does not necessarily result in exocyclic binding and endocyclic binding is observed

even for relatively rigid ligands. For example, Lee and co-workers treated DB[20]ene-O_4S_2 ligand **7** (Figure 18) with a variety of different metals and observed several different structures and coordination modes that depended on the metal used. In the case of $Pb[ClO_4]_2 \cdot 3H_2O$, the reaction afforded an *endocyclic* mononuclear perchlorate complex $[Pb(\mathbf{7})][ClO_4]_2$ (**8**) (Figure 19, POFYUG).[86] Complex **8** features a "tight and bent" conformation with a geometry that can be best described as a distorted hexagonal bipyramid. The authors rationalized that the endocyclic preference in the case of Pb^{2+} can be explained by the intermediate softness of Pb^{2+} – it is characterized as lying roughly intermediate between a soft and a hard acid – but, as noted above, endocyclic binding is observed for almost every polyether with a large enough cavity.[86]

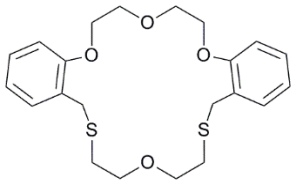

Figure 18. Ligand **7**.

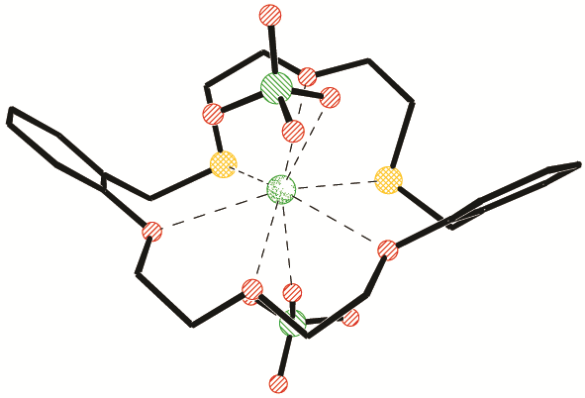

Figure 19. Compound **8** ($[Pb(\mathbf{7})][ClO_4]_2$) – POFYUG

Braga and co-workers reported a clear demonstration of the use of anion interactions and hydrogen bonding to generate a designed coordination polymer network. They found that the that

manual grinding of [18]crown-6 with $PbSO_4$ in the presence of H_2SO_4 (in a 1:1:2 ratio, respectively) resulted in the coordination polymer $([Pb([15]crown-5)][HSO_4]_2)_n$ **9** (Figure 20, SIDKUM).[87] The as-prepared material **9** is polycrystalline and recrystallization from water results in pure crystals of the coordination polymer. The network features $[Pb([18]crown-6)]^{2+}$ cationic fragments that are linked by dimeric hydrogen bonded $[HSO_4]_2^{2-}$ unit, as shown in the figure.

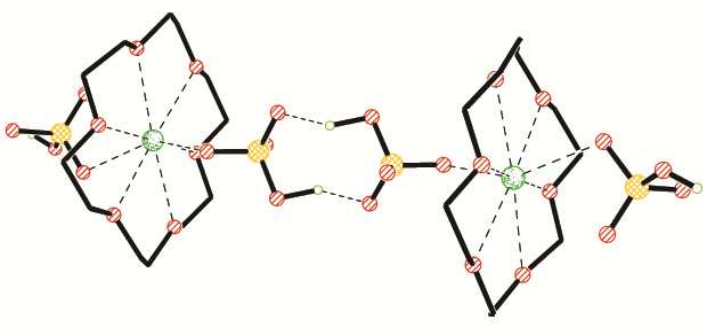

Figure 20. Compound **9** ($[Pb([15]crown-5)][HSO_4]_2$) – SIDKUM

Mullen and Chen[88] recently reported a dibenzocoronene tetracarboxdiimide macrocycle containing two benzo-[21]crown-7 groups (ligand **10**, Dibenzo-CDI, Figure 21). Treatment of the macrocycle with two equivalents of lead(II) or potassium(I) leads to the complexation of metal ions to each of the [18]crown-6 cavities. Such complexation results in a significant increase in the fluorescence of the molecule and to a change in the molecular packing of this self-organizing macrocycle. They screened this macrocycle with different heavy metal ions (including nickel(II), cobalt(II) and others) and found that changes in the fluorescence response only occur for complexes of lead(II) and potassium(I). They found that the increase in fluorescence continues until two molar equivalents of the metal ion are added. Grazing-incidence wide-angle X-ray scattering (GIWAXS) indicates that the π-stacking organization of the free dibenzo-CDI ligands features a spacing of 3.5 Å between adjacent ligands. This spacing increases to 3.8 Å and 3.7 Å upon the complexation of potassium(I) and lead(II) ions, respectively, as one would anticipate given the larger size of the potassium(I) ion.

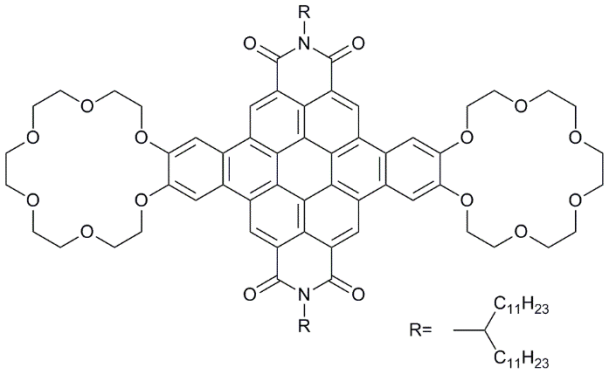

Figure 21. Dibenzo CDI, **10**.

Ilhan[89] reported that the treatment of the Schiff base macrocycle **11** (Figure 22) with different metal nitrates (Pb(II), Zn(II), Cd(II) and La(III)) results in the complexation of the metal ions to **11** in a 1:1 molar ratio. The complexes were characterized and analyzed by elemental analysis, FT-IR, UV-Vis, molar conductivity measurements, NMR and mass spectrometry and related work by the same group probed the coordination chemistry of similar Schiff base macrocycles.[89-97]

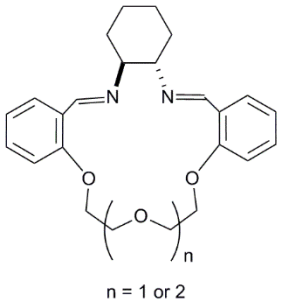

Figure 22. Compound **11**.

Vila and Fernández[98] also prepared a crown ether ligand featuring a Schiff base, but the imine fragment was not part of the ring. Instead, they used a cyclometalation reaction of aryl-imine fragment with $Pd(OAc)_2$ to produce a dimeric ligand with two crown ether groups. Treatment of the dimeric ligand with lead(II) thiocyanate, results in the coordination of lead(II) to the crown ether moieties (Scheme 6). Screening of the ligand was performed with different cations (Na^+, K^+, NH_4^+, Pb^{2+}, Rb^+ and

Ba^{2+}) using both [18]crown-6 and [15]crown-5 based ligands but only the [15]crown-5 sodium(I) complex resulted in crystals suitable for X-ray diffraction. The remaining compounds were characterized by elemental analysis and mass spectrometry. The results demonstrated the viability of this ligand system to prepare mixed transition metal-main group metal tetrametallic complexes.

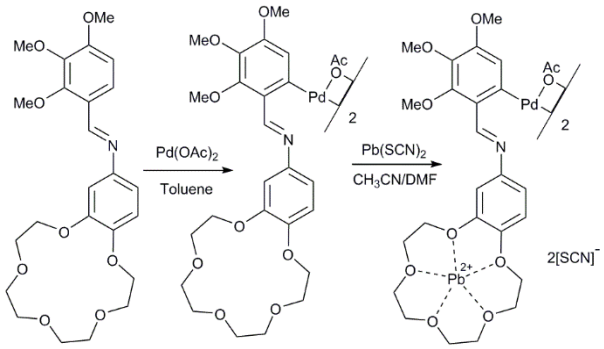

Scheme 6. Reaction scheme showing the cyclo-metallation of palladium followed by the complexation of lead(II) in the crown moiety.

Scheme 7 contains a selection of other lead(II) polyether complexes reported in literature that exhibit features worthy of note. The complexes **12**[99] and **13**[100] were reported by Ertul and co-workers and feature lead(II) bound by the calixarene-crown ether hybrid macrocycles illustrated in the scheme. In both cases, the lead(II) complexes were characterized by elemental analysis.

Bernes and co-workers reported compound **14**, which was obtained by treatment of the aza-crown ether shown with $Pb(NO_3)_2$ in aqueous media and in the presence of picric acid.[101] The picric acid serves as both an anion and as a co-ligand which enhances the extraction of lead(II) from solution. The compound has been characterized by scXRD (LEPHIY) and the crystal structure reveals that one of the picric acid anions is coordinated closely to the lead(II) center. This sort of arrangement in which an auxiliary donor sidearm (e.g. ketone/fluoride) is appended to the nitrogen atom in the macrocycle is

common, as illustrated by the complexes reported by Sazonov[102, 103] (**17**, ELUJEB; **18**, DOSHUP), and Valencia[104, 105] (see IDAVEP, **15**).

Mahbubul reported the synthesis of a Schiff base polyether ligand that was prepared by the condensation of pyridine-2,6-dicarboxaldehyde with 1,2-bis(2-aminoethoxy) ethane.[106] The author postulated that this macrocycle should large enough to extract two lead(II) metal centers per ligand. Treatment of the ligand with two equivalents of $Pb[SCN]_2$ in Et2O at 50°C resulted in the formation of **16** as yellow crystalline material. The composition of this material was confirmed by elemental analysis and was found to be consistent with the presence of two lead(II) centers per ligand.

Fedorova and co-workers reported the synthesis of complex **19** in which the lead(II) center is found to be in an equilibrium between forms in which the metal is bound by either the crown ether fragment or the ketone-imine fragment.[107] They discovered that complexation of the lead(II) center to the ketone (when kept in the dark) induces the formation of an oxazole derivative in a manner that is both irreversible and regioselective.

Su reported the lariat crown ether complexes **19a**-**c** which were prepared for the purpose of probing the energetics associated with the binding and conformations adopted by the different ligands.[108] The structures were determined using scXRD studies and the thermodynamic values associated with the different ligands and their conformations were investigated using several DFT methods. The computational results indicate that the ligand featuring the ether sidearm forms the most stable complexes with lead(II).

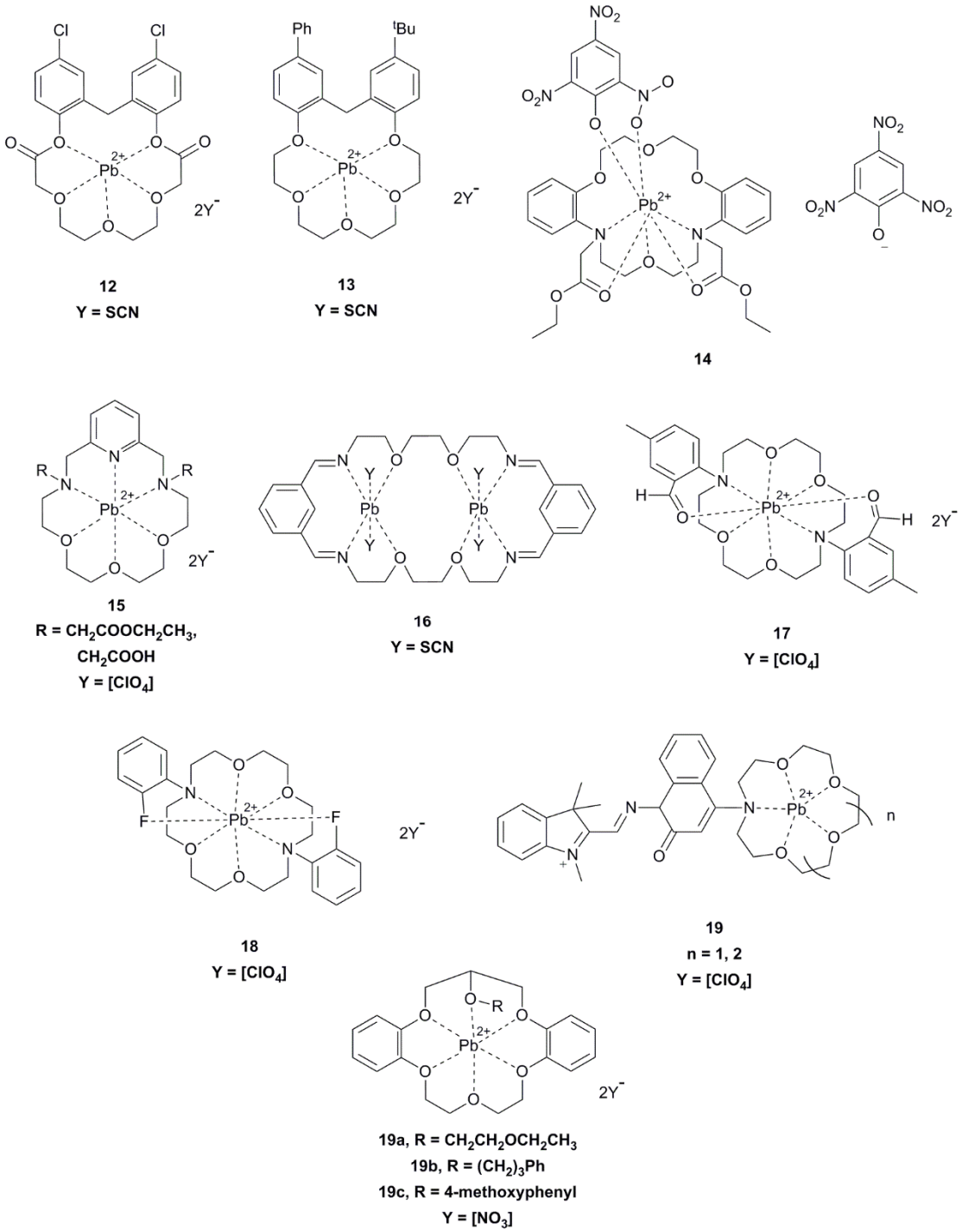

Scheme 7. Selection of other noteworthy lead(II) polyether complexes.

Finally, from a somewhat different perspective, Mizuno and co-workers reported the crystal structure shown in Figure 23 (TUDHEG) in which two lead(II) centers are encapsulated in a

polyoxometallate compound that they describe as an inorganic cryptand.[109] Complexes of both lead(II) and strontium(II) were reported and, in order to study the strength of the coordination associated with the inorganic cryptand, both complexes were treated with crypt[2.2.1]. For strontium(II), they found the first example of a system in which an inorganic cryptand encapsulates a metal center more strongly than an organic cryptand. In contrast, they found that exposing the lead(II) inorganic cryptand complex to the crypt[2.2.1] resulted in the transfer of the lead(II) center to the organic cryptand.

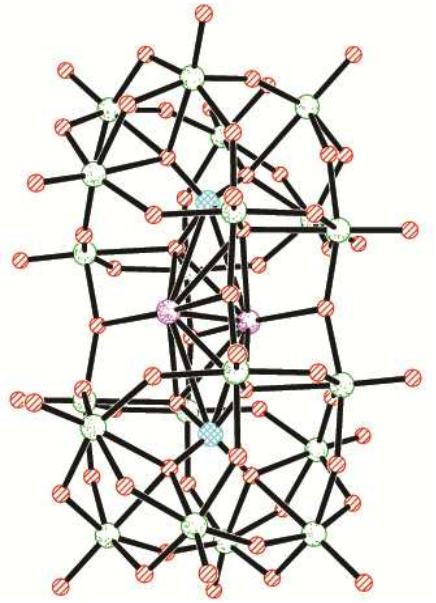

Figure 23. Lead(II) center bound to the inorganic cryptand disilicoicosatungstate (Si_2W_{20}) polyoxometalate (TUDHEG).

2.1.2 Lead(IV)

There do not appear to be any structurally authenticated complexes of lead(IV) with crown ethers or the other types of ligands described above.

2.2 Tin

The relative stability of both tin(II) and tin(IV) has allowed for the isolation of polyether complexes containing the metal in each of the oxidation states but considerably more compounds have been prepared with tin(II).

2.2.1 Tin(II)

$SnCl_2$ is commonly used as a reducing agent and often undergoes insertion into element-halogen or metal-halogen bonds to produce synthetically useful metal stannyl species.[110] The reaction of SnX_2 with palladium and platinum has been studied and reported extensively but only a few examples of ruthenium complexes containing trichlorostannyl ligands have been reported.[111] Fink and co-workers found that $[(\eta^6\text{-}Pr^iC_6H_4Me)Ru(\mu_2\text{-}Cl)Cl]_2$ reacts with an excess of $SnCl_2$ and two equivalents of [18]crown-6 in refluxing ethanol to yield $[SnCl([18]crown\text{-}6)][(\eta^6\text{-}Pr^iC_6H_4Me)Ru(SnCl_3)_2Cl]$ (Figure 24, BULDUI) as shown in Scheme 8.[112] As demonstrated in the following paragraphs, the $[SnCl([18]crown\text{-}6)]^+$ is a very common entity in the crown ether chemistry of tin(II) and it features a "pin-wheel" structure in which the Sn-Cl fragment is roughly perpendicular to the O_6 plane. The metrical parameters in this cation are typical of such ions; the Sn-Cl distance is 2.3978(11) Å and the Sn···O distances range from 2.597(3) to 2.872(3) Å.

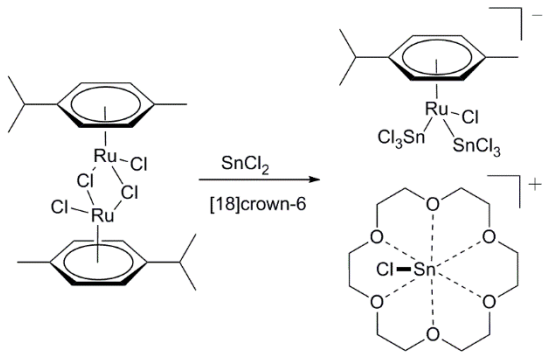

Scheme 8. $SnCl_2$ used as a reducing agent which results in the crown ether complex cation shown.

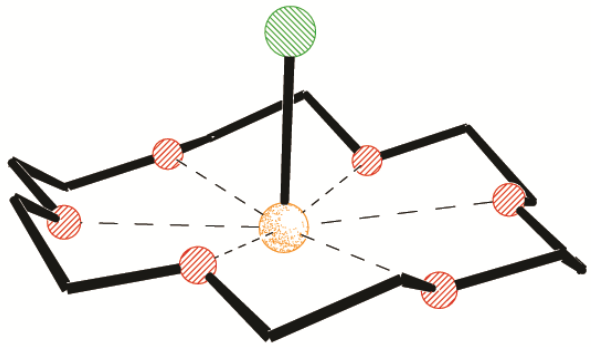

Figure 24. [SnCl([18]crown-6)]$^{+}$ – BULDUI

In a similar vein, Pasynskii[113] and co-workers reported that the treatment of (Dppm)$PtCl_2$ with $SnCl_2 \cdot 2H_2O$ in DCM/EtOH in presence of diglyme results in [(diglyme)SnCl][(Dppm)Pt as a yellow solid (Scheme 9). In the same paper, Pasynskii reported the synthesis of different metal-tin complexes featuring platinum, iron and manganese but only the platinum-containing salt yielded material suitable for scXRD characterization. It is worth noting that the changes in the spectral features of acyclic polyethers such as diglyme upon complex formation are more pronounced and diagnostic than are those of crown ethers.

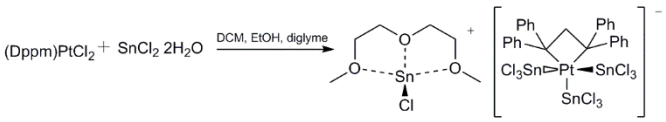

Scheme 9. Synthesis of [(diglyme)SnCl][(Dppm)Pt.

As indicated above, iodometallates such as iodostannates are of particular interest for their semiconductor properties.[114] Potential applications of these iodostannates include photovoltaics, thermoelectrics and high-power batteries.[115] Feldmann and co-workers reported that the reaction of SnI_2 and SnI_4 in the presence of [18]crown-6 in [NMe(^{n}Bu)$_3$][N(Tf)$_2$] results in a material with the overall

composition: Sn_3I_8·2([18]crown-6), which exits as the mixed valent tin(II)-tin(IV) salt [(SnI([18]crown-6))$_2$(μ^2-I)][SnI_5] (Figure 25, COYPIQ). The structure of the cation is analogous to the one described above for lead(II) and features two [SnI([18]crown-6)]$^+$ cations linked by a bridging iodide anion. The terminal Sn-I distances of 2.872(1) Å are shorter than the 3.552(1) Å distance to the bridging iodide and all of the Sn···O distances (2.612(1) – 2.937(1) Å) fall within the range. Again, the choice of the ionic liquid solvent was to provide the reaction with a polar but aprotic environment which would provide a fast diffusion of the reactants.

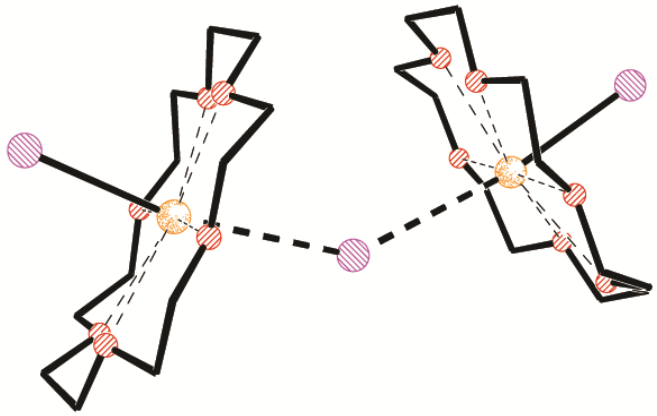

Figure 25. [(SnI([18]crown-6))$_2$(μ^2-I)]$^+$ – COYPIQ

[SnCl([18]crown-6)][$SnCl_3$] and [Sn([15]crown-5)$_2$][$SnCl_3$]$_2$ (KAYJOJ) had been previously reported and crystallographically characterized.[116, 117] Macdonald and co-workers later reported the complexation of tin(II) triflate to different crown ethers.[118, 119] As one would anticipate, different crown ethers resulted in different modes of coordination to the tin(II) center (Figure 26**,** XULKOF, VUTJAW and VUTHUO). Treatment of Sn[OTf]$_2$ with [18]crown-6 yielded compound **20A** with the tin(II) atom belted in a *mer* conformation by the crown ether. Smaller crown ethers such as [15]crown-5 and [12]crown-4 yielded sandwich-like structures (**20B** and **20C**) in which two of the crown ethers coordinate to one tin(II) center. The Sn···O distances in **20A** range from 2.464(6) – 3.026(6) Å and the pattern of four

shorter bonds and two longer bonds highlights the off-center location of the tin atom and suggests that the Sn^{2+} ion appears to be smaller than those in the $[SnX([18]crown-6)]^{+}$ cations described above. The roughly centrosymmetric dication in **20B** has Sn···O distances that range from 2.53(2) – 2. 98(1) Å and those in the bent sandwich cationic portion of **20C** are similar: 2.474(3) – 2.813(3) Å. Perhaps the most interesting aspect of this series of compounds is the nature of the anion interactions. Although **20A** features the relatively short interaction 2.282(9) Å with one of the two triflate ions, the metrical parameters within the triflate indicate that it is ionic so this is likely a contact ion pair; the absence of a close interaction on the opposite face of the complex could allow for the presence of a stereochemically active pair of non-bonding electrons. In the sandwich complexes, there are clearly no Sn···OTf interactions possible in **20B** but the bent arrangement in **20C** allows for a potential Sn···OTf interaction. The actual Sn···OTf distance of 3.119(4) Å suggests that this interaction is not strong but the orientation of the anion suggests that the bending in the cation should not be attributed to the presence of a stereochemically active pair of non-bonding electrons.

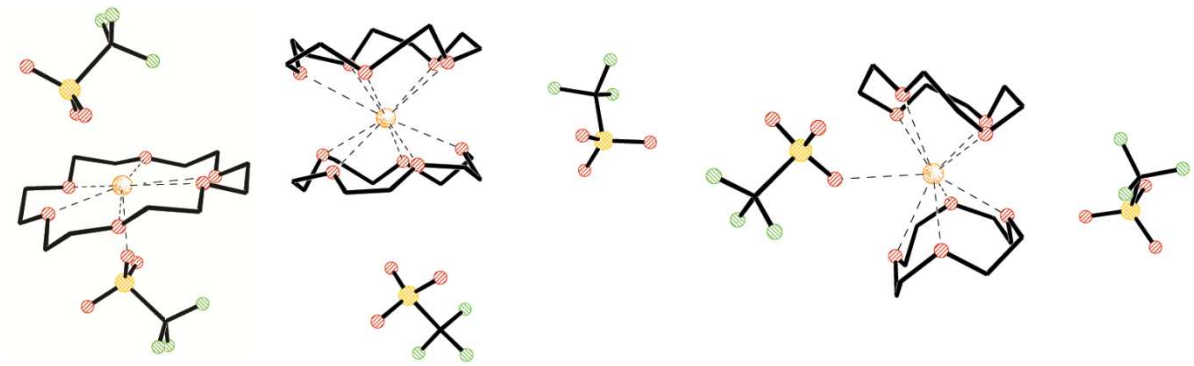

Figure 26. Different tin(II) compounds resulting from the reaction of $Sn[OTf]_2$ with different crown ethers. From left to right, compound **20A** (XULKOF), **20B** (VUTJAW) and **20C** (VUTHUO).

In light of the obvious importance of the size of the crown ether in regard to the structure observed for the resultant tin(II) complexes, Macdonald and co-workers investigated the use of glymes,

which are acyclic polyethers that are flexible and lack the cyclic constraints of crown ethers. Treatment of $Sn[OTf]_2$ with triglyme or tetraglyme in acetonitrile yielded $Sn(OTf)_2$triglyme (also denoted as $Sn(OTf)_2$@triglyme) (HATCOW) and $Sn[OTf]_2$tetraglyme (also denoted as $Sn(OTf)_2$@tetraglyme) (HATCIQ) quantitatively (Figure 27). In each complex, the glyme ligand binds the tin(II) atom in a *mer* conformation with Sn···O distances that range from 2.378(3) – 2.968(5) Å and each complexes can also be described as containing contact ion pairs of Sn^{2+} and triflate anions.

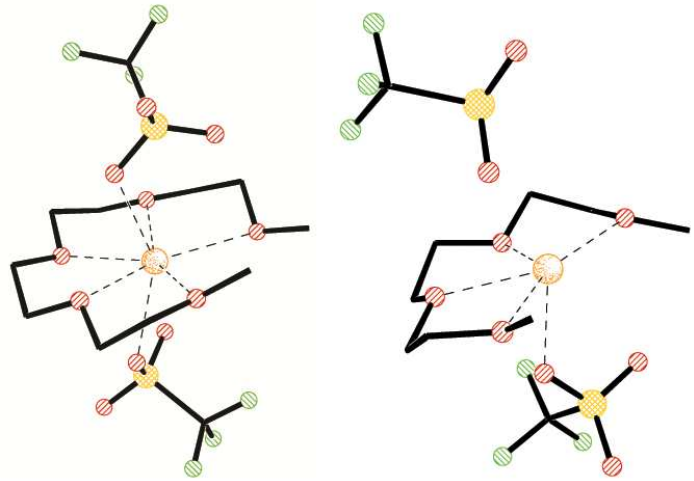

Figure 27. $Sn[OTf]_2$tetraglyme (left) – HATCIQ and $Sn[OTf]_2$triglyme (right) – HATCOW

An extensive investigation of the crown ether and glyme bound complexes of $Sn[OTf]_2$ and $[SnCl([18]crown-6)][SnCl_3]$ using solid-state ^{119}Sn NMR spectroscopy, ^{119}Sn Mössbauer spectroscopy, electrochemistry, and DFT and MP2 computational studies of these compounds gave insight onto the nature of the symmetry, electric field gradient, charge distribution, electronic structure and binding in such complexes. The results demonstrated that the sandwich complex **20B**, which exhibits the most spherical distribution of oxygen atoms around the tin cation, has the most $5s^2$ character: it features the most shielded ^{119}Sn NMR chemical shift (ca. –1700 ppm); it has the largest ^{119}Sn Mössbauer isomer shift (4.504(6) mm s^{-1}), with a quadrupolar splitting of 0.0(1), it is not readily oxidized; and the calculations suggest that the non-bonding valence electrons have an s-character of more than 99%. The

investigations indicated that deviations from spherical symmetry do indeed result in the destabilization of the non-bonding electrons on tin; such deviations can be controlled by the choice of polyether used to prepare the complex. More dramatic changes result from choice of counter ion: whereas triflate salts are primarily ionic in nature – perhaps featuring contact-ion-pair (or charge shift bonding[120]) interactions – the much more covalent binding of chloride ions results in considerably more localization and destabilization of the non-bonding electrons.[118, 119] An important conclusion that was drawn from these results is that the bonding and chemistry of superficially similar complexes, such as $[SnCl([18]crown-6)]^+$ and "$[SnOTf([18]crown-6)]^+$" can be dramatically different.

Baines and co-workers investigated the chemistry cryptand complexes of group 14 elements and their work included the synthesis and characterization of the first tin(II) cryptand complexes.[121] Treatment of crypt[2.2.2] with SnX_2 in THF resulted in the complexes shown in Scheme 10 (QEKJOH, QEKJUN and QEKKAU). Mössbauer spectroscopy spectra of these compounds consisted of well-resolved doublets (distinctive for ^{119}Sn) and isomer shifts consistent with the tin(II) oxidation state (ranging from 4.21(2)-4.40(2) mm s^{-1}). Solid-state ^{119}Sn NMR investigations were consistent with the results observed for the crown ether complexes investigated by Macdonald and co-workers.[119] Interestingly, tin(II) appears to be too large to become fully encapsulated by the cryptand, thus, the resulting complexes adopt pinwheel-like (or perhaps umbrella-like) structures in the solid state, as illustrated by the chloride complex example $[SnCl(crypt[2.2.2])]^+$ in Figure 28 (QEKJOH).

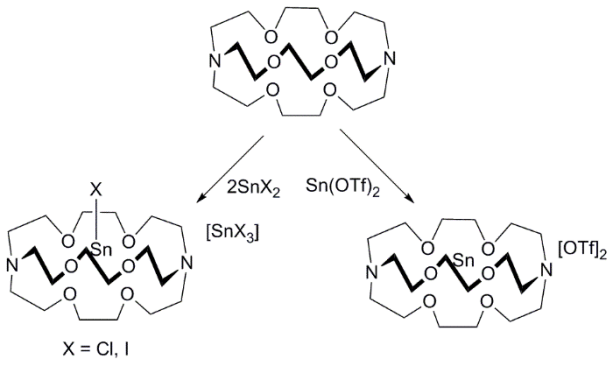

Scheme 10. crypt[2.2.2] reaction with different tin(II) starting materials.

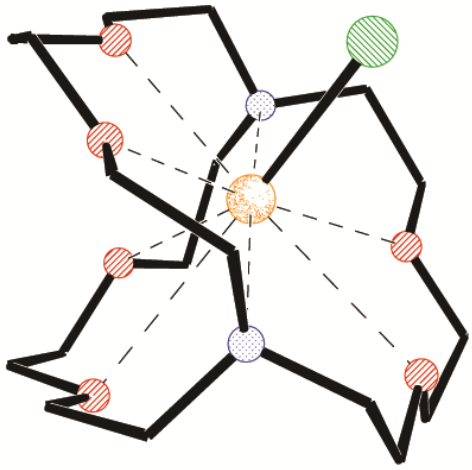

Figure 28. $[SnCl(crypt[2.2.2])]^{+}$ – QEKJOH

Reid and Levason[122] recently reported different tin(II) complexes from reactions of freshly prepared solutions of $Sn[BF_4]_2$ or $Sn[PF_6]_2$ with different crown ethers. Treatment of $Sn[BF_4]_2$ with [15]crown-5 in wet solutions of acetonitrile yielded a sandwiched complex $[Sn([15]crown\text{-}5)_2][BF_4]_2$ which recrystallized as a co-crystal with the formula $[Sn([15]crown\text{-}5)_2][H_3O][BF_4]_3{\cdot}H_2O$ (XIJHUV); the tin-containing cation is shown in Figure 29 (XIJHUV). Treatment of $Sn[BF_4]_2$ with [18]crown-6 on the other hand yielded a "belted" *mer*-like structure $[Sn([18]crown\text{-}6)(H_2O)][BF_4]_2{\cdot}2H_2O$ (XIJHOP) with a 1:1 metal/ligand complexation. Note that in the XIJHUV structure, the water does not coordinate to the tin(II) center, while water coordination is observed in the [18]crown-6 structure (XIJHOP). This observation is similar to prior reports,[66, 67, 118, 119] wherein crown ethers smaller than [18]crown-6 tends to adopt a sandwich like structure with a 1:2 metal/ligand complexation, while [18]crown-6 adopts a belted structure with a 1:1 metal/ligand complexation. $Sn[PF_6]_2$ exhibited slightly different reactivity towards crown ethers: the $[PF_6]^{-}$ anion readily undergoes hydrolysis to liberate an F^{-} anion that binds to the tin center generating $[SnF([18]crown\text{-}6)][PF_6]$ (Figure 30, XIHTEP), which contains an pinwheel-like

structure analogous to those observed for the heavier halides described above.[122] Interestingly, the analogous reaction of $Sn[BF_4]_2$ with [18]ane-O_4S_2 yielded the salt $[Sn([18]aneO_4S_2)(HOCH_2CH_2OH)][BF_4]_2$ (XIJJAD) in which the polyether ligand had clearly been decomposed to produce the ethylene glycol ligand.

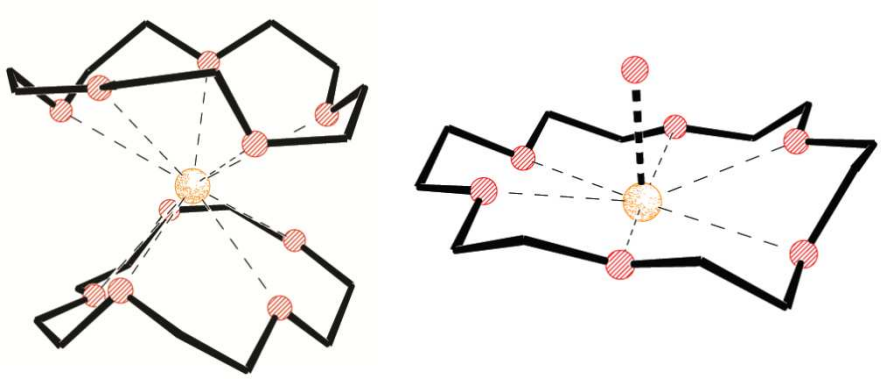

Figure 29. Left: $[Sn([15]crown\text{-}5)_2]^{2+}$ – XIJHUV; the water molecules do not interact directly with the tin atom; Right: $[Sn(OH_2)([18]crown\text{-}6)]^{2+}$ – XIJHOP; hydrogen atom positions for the water molecule are not in the CSD record.

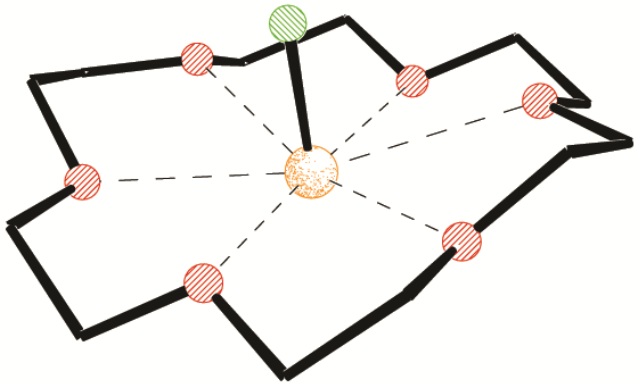

Figure 30. $[SnF([18]crown\text{-}6)]^{+}$ – XIHTEP

Jurkschat[123] and Sarazin[124, 125] reported the coordination of different aza-polyether fragments of the form [12]ane-O_3N or [15]ane-O_4N to tin(II), lead(II) and germanium(II). In the case of tin(II), $^{119}Sn\{^1H\}$ NMR spectroscopy was used extensively to study and identify different components of the reaction.

They found that the treatment of $Sn[NMe_2]_2$ with 1 equivalent of **21-H** (Figure 31) results in [**21**]Sn-NMe_2 which exhibits a $^{119}Sn\{^1H\}$ NMR chemical shift at δ = −147 ppm, whereas the treatment of the tin starting materials with 2 equivalents of **21-H** results in $[\mathbf{21}]_2Sn$ which has a much more shielded $^{119}Sn\{^1H\}$ NMR chemical shift at δ = −566 ppm. As can be inferred by the stoichiometry and the observation of easily observed signals in the ^{119}Sn NMR, the complexes do not contain tin(II) encapsulated within the aza-crown ether but are best considered as phenolic stannylenes. Other tin and ligand starting materials were investigated and the results indicated that the presence of these low-coordinate cationic tin(II) centers adjacent to the macrocyclic fragment(s) can engender enhanced or unusual reactivity that they exploited further for lactide polymerization. These results are discussed is more detail below in the germanium(II) section.

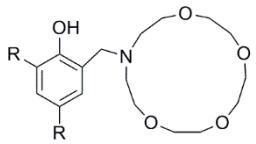

21-H

Figure 31. An aza-polyether fragment ligand, **21-H**.

2.2.2 Tin(IV)

Atwood and co-workers reported much of the earlier work in regard to the preparation and structural details of tin(IV) crown ether complexes. For example, the treatment of [18]crown-6 with $SnCl_4$ in toluene, provided the complex shown in Figure 32 (KAVKIB).[126] As illustrated in the figure, the coordination of tin(IV) is typically exocyclic to the crown due to the steric constrains of chlorides. There is, however, one report of a related glycol complex, derived from the decomposition of [15]crown-5 by $SnCl_4$, with the general formula $Sn_2Cl_6(O_4C_8H_{16})_5$ (SEFZAE) in which a linear $Sn^{IV}Cl_2$ fragment is bound in an endocyclic manner by the polyether, as illustrated in Figure 33. [127]

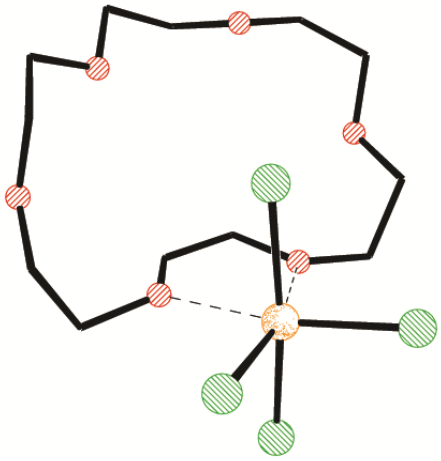

Figure 32. $[SnCl_4([18]crown-6)]$ – KAVKIB

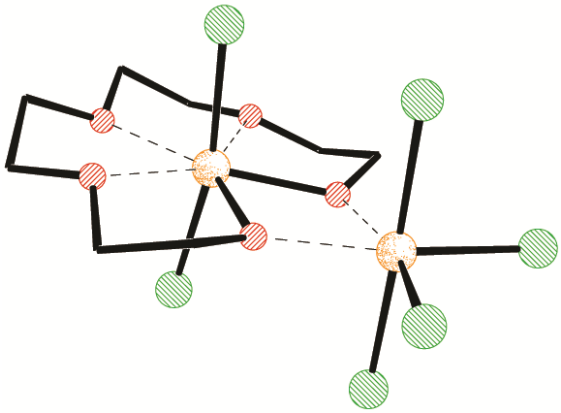

Figure 33. $Sn_2Cl_6(OCH_2CH_2)_5$ – SEFZAE

More recently, Jurkschat and co-workers showed that treating related tin(IV) complexes in which the Sn atom is tethered to the ring with $Ag[ClO]_4$ or Ag[OTf] (Scheme 11) results in sufficiently weakly-coordinating anions which would allow the tin(IV) to fit in the crown ether pocket as shown in Figure 34.[128] When other corresponding tin(IV) halides are used, the tin atom is bound invariably in an exocyclic manner.[123] The use of such tin(IV) species as ditopic acceptors for alkali metal salts – in which the alkali metal cation is bound by the polyether and the anions binds to the tin(IV) center – has been

demonstrated and even bis(crown ether) tin(IV) acceptors (Figure 35, SIGHUN) have been prepared.[129, 130]

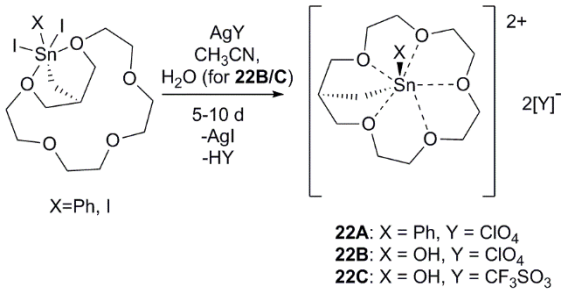

Scheme 11. Treatment of an externally bound Sn(IV) with AgY (Y = ClO_4 or CF_3SO_3) results in the coordination of Sn(IV) in cavity of the crown ether.

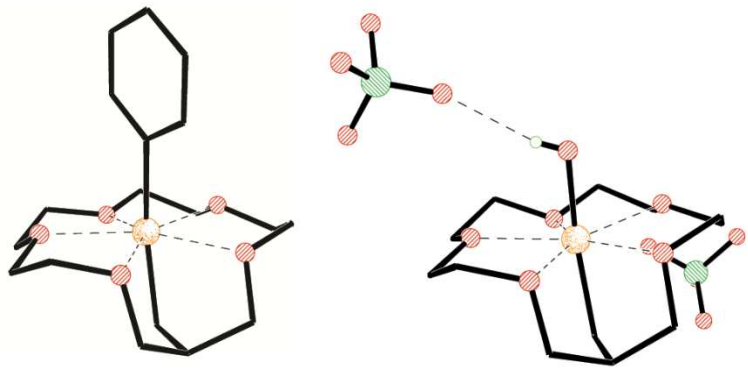

Figure 34. Left: $[PhSnCH_2([16]crown\text{-}5)]^{2+}$ – BACSIJ; Right: $[(OH)SnCH_2([16]crown\text{-}5)][ClO_4]_2$ – BACSEF

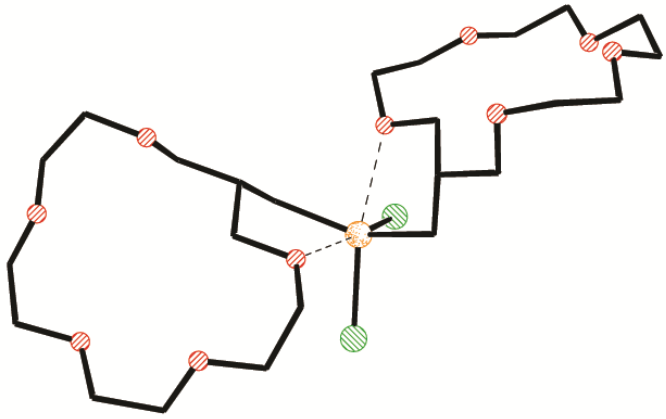

Figure 35. $Cl_2Sn(CH_2–[16]crown\text{-}5)_2$ – SIGHUN

Pettinari and co-workers used oxydiacetate anions (oda^{2-}) derived from oxydiacetic acid ($odaH_2$; Figure 36) to bind tin(IV) cations. Although it is not really a polyether, this type of ligand is comprised of five potential oxygen donor atoms and such ligands have been widely investigated as bridging and chelating entities. [131, 132] Pettinari reported that the reaction of R_2SnCl_2 (where R = Me, ^{n}Bu or Ph) with $odaH_2$ (Figure 36) and 2 equivalents of KOH in methanol resulted in the compound $[Me_2Sn(oda)(H_2O)]_2$, which exhibits the dimeric structure shown in Figure 37 (GAMYID). They found that even under identical conditions, the analogous reactions in which the substituent (R) on tin is Et, ^{i}Bu or ^{t}Bu results instead in the production of polymeric materials with different metal to ligand ratios. They postulated that the polymeric structure results from the steric hindrance enforced by the bulkier R groups, which inhibits complete substitution of the chloride ions by the oda^{2-} ligand.[133]

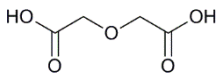

Figure 36. oxydiacetic acid, $odaH_2$.

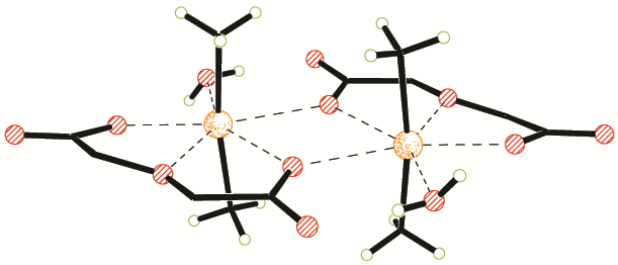

Figure 37. $[Me_2Sn(oda)(H_2O)]_2$ – GAMYID

2.3 Germanium

Perhaps as a consequence of the more metallic nature of lower oxidation state ions, all of the structurally characterized polyether complexes contain germanium(II).

2.3.1 Germanium(II)

The isolation and characterization of the complex $[Ge(crypt[2.2.2])][OTf]_2$ (VOMLAL)[134] was a landmark in main group chemistry. In general, germanium centers require covalent bonds with ligands to form stable compounds and no simple coordination complex of the germanium(II) ion had been reported previously.[20, 134] Baines and co-workers reported that the treatment of cryptand ligand crypt[2.2.2] with the reagent NHC-$GeCl(O_3SCF_3)$ generated the salt $[Ge(crypt[2.2.2])][OTf]_2$ (Figure 38, VOMLAL).[134] Because of the unprecedented nature of the cation, the authors used EDX experiments in order to confirm that the ion contained within the cryptand was indeed germanium. The Ge···N and Ge···O distances in the crystal structure are 2.524(3) and 2.4856(16) Å respectively which are much longer than the typical Ge–N and Ge–O distances of 1.85 and 1.80 Å respectively.[135, 136] The structural data, in conjunction with NBO analyses were consistent with absence of substantial covalent bonding

between the cryptand and the Ge^{2+} ion. Subsequent investigations with XANES[129] confirmed the highly ionic nature of the bonding between the cryptand and the germanium ion within the cation of the salt.

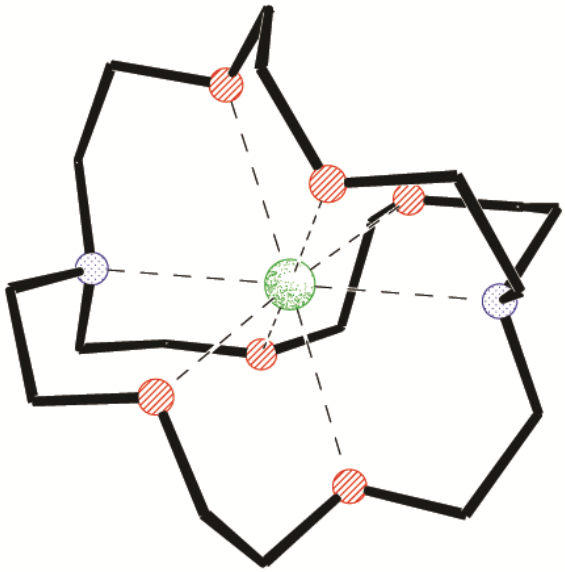

Figure 38. [Ge(crypt[2.2.2])][OTf]$_2$ – VOMLAL

Simultaneous reports by the groups of Reid[137] and Baines and Macdonald[138] subsequently demonstrated that similar "free" Ge^{2+} ions can also be stabilized by crown ethers. In particular, both groups reported salts of the dication $[([12]crown\text{-}4)_2Ge]^{2+}$ featuring counter anions of $[GeBr_3]^-$ (XULLIA), $[GeCl_3]^-$ (XULKAR) or $[OTf]^-$ (RUPMUL). The salts are each produced in high yield by the treatment of "GeX_2" (X = Cl, Br, OTf) with appropriate ratios of [12]crown-4. There are no unusually strong contacts between the cations and anions in these salts so structure of the dication is similar in each instance. As illustrated in Figure 39, the dication consists of a roughly centrosymmetric "sandwich-like" complex and features Ge···O distances ranging from around 2.284(9) – 2.489(8) Å and there is no evidence for the presence of a stereochemically active lone pair of electrons. These important observations illustrated that the rigorous geometrical constraints of a cryptand are not required in order to isolate Ge^{2+} ions.

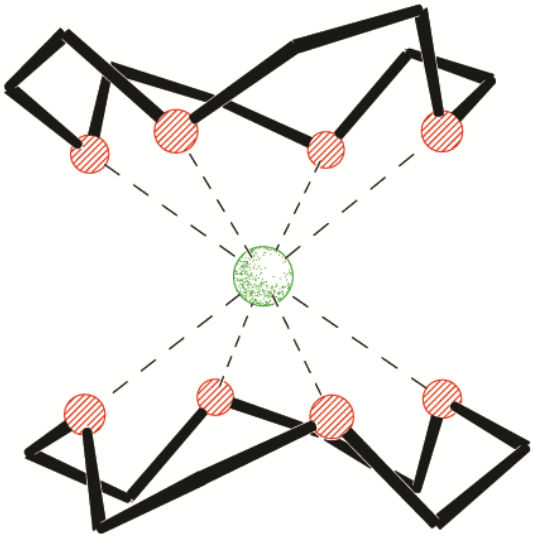

Figure 39. $[([12]crown\text{-}4)_2Ge]^{2+}$ featuring counter anions of $[GeBr_3]^-$ (XULLIA), $[GeCl_3]^-$ (XULKAR) and $[OTf]^-$ (RUPMUL).

In their report, Reid and co-workers also demonstrated that cyclic polyamine donors are also able to generate complexes of Ge^{2+}. The crystal structures of the salts $[Ge(Me_4\text{-cyclam4})][GeBr_3]_2$ and $[Ge(Me_3\text{-cyclam3})][Br][GeBr_3]$ (XULLEW) contain cations with very long Ge···N distances ranging from 2.124(3) – 2.349(2) Å, which are considerably longer than those found in related cyclam adducts of germanium(IV) (e.g. the Ge-N distance in the complex $[GeF_3(Me_3\text{-cyclam3})][Cl]$ is 2.043(3)Å.[139] Both cations are "half sandwich" complexes that feature distinctly pyramidal geometries about the germanium atom that allow for the presence of a stereochemically active lone pair of electrons.

In terms of additional polyether chemistry, the groups of Baines and Macdonald also characterized the adducts of germanium(II) chlorides and triflates with larger crown ethers, which also produced ions with a 1:1 ratio of ligand to metal but that exhibited considerable structural variation depending on the counter ions present. For example, treatment of 2 equivalents of $GeCl_2$·dioxane with [15]crown-5 produces the salt $[([15]crown\text{-}5)GeCl][GeCl_3]$ (XULJOE), in which the cation (Figure 40, XULJOE). The salt features a monocationic Ge-Cl fragment that is coordinated by a crown ether

exhibiting an unusual "folded" (*fac*-like) arrangement and that has one relatively short Ge···O distance of 2.104(6) Å. Overall, the geometrical features appear to be consistent with the presence of a stereochemically active lone pair and a germylene-like structure.

In contrast to [([15]crown-5)GeCl][$GeCl_3$], the appearance of the cation in the related triflate salt [([15]crown-5)Ge][$OTf]_2$ (XULKEV) is very different, and features a more conventional (*mer*-like) crown ether arrangement, as illustrated in Figure 41 (XULKEV). One of the triflate anions in the salt is in relatively close proximity to the Ge atom so the salt could perhaps also be formulated [([15]crown-5)GeOTf][OTf], but the metrical parameters within the triflate suggest that it is largely ionic in nature and the Ge···O distance of 2.015(3) Å is still much longer than those of typical covalent Ge-O bonds. Thus the Ge···O interactions is perhaps best considered as a contact ion pair (or as an example of charge-shift bonding[120]). The structural features of the analogous cations bearing benzannulated crown ethers, namely [Ge(B[15]crown-5)][$OTf]_2$ (RUPNAS), and [GeCl(B[15]crown-5)][OTf] (XULJIY), show similar structural features and suggest that the different modes of crown ether binding are not likely attributable to packing effects.

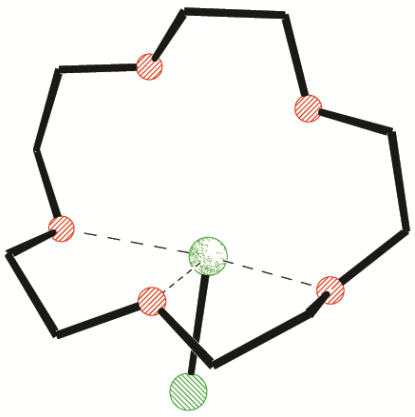

Figure 40. [GeCl([15]crown-5)]$^+$ – XULJOE, illustrating the "folded" (*fac*-like) arrangement of the [15]crown-5 ligand; the GeO_3 unit indicated by the dashed lines is approximately 90° from the GeO_2 plane defined by the two remaining O atoms in the ring.

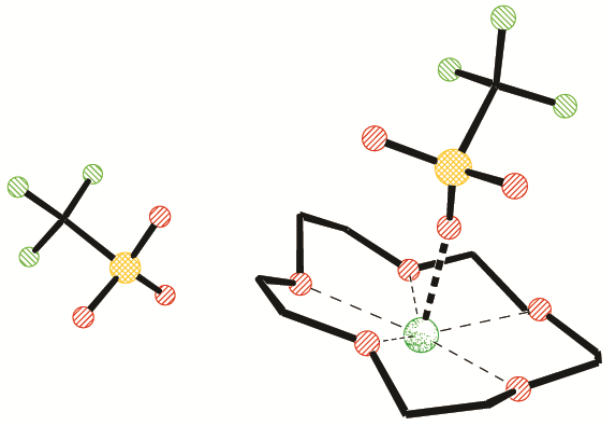

Figure 41. [Ge([15]crown-5)][OTf]$_2$ – XULKEV, showing the more common *mer*-like arrangement of the [15]crown-5 ligand.

The complexes with the larger [18]crown-6 polyether exhibit a similar speciation (Figure 42, XULJUK): the chloride variant [GeCl([18]crown-6)][GeCl$_3$] (XULJUK) features an unambiguously monocationic fragment that is complexed in a *mer*-like fashion by the crown ether whereas the triflate salt [Ge([18]crown-6)][OTf]$_2$ (XULKIZ) has two anions with very long contacts Ge···O of 2.204(5) Å. It is noteworthy that the structures of both of the [18]crown-6 complexes exhibit features that reveal that neither of the germanium(II) ions fill the cavity completely; in each salt, the germanium ion is not situated at the centroid of the O_6 ring but is near one end of the [18]crown-6 ligand. Overall, the authors suggested that the data are consistent with the existence of larger monocationic [Ge–Cl]$^+$ ions – which appear to be too big to fit within the cavity of [15]crown-5 rings in the chloride-bearing salts – and smaller Ge^{2+} dications, which do fit within such rings, in the triflate salts.[138] The conclusion about the differing nature of the analogous halide and triflate species is in accord with the physical and spectroscopic investigations on related tin(II) complexes described in a previous section. It is worth noting that some of the chloride-containing polyether salts were subsequently used for ^{35}Cl solid-state NMR investigations in order to develop an indirect method to assign the oxidation state of germanium.[140]

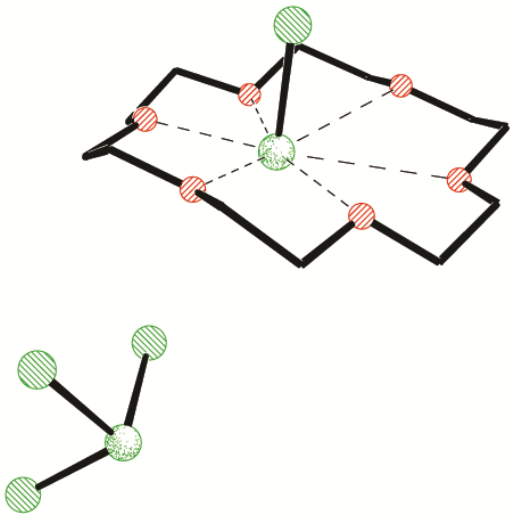

Figure 42. [GeCl([18]crown-6)][$GeCl_3$] – XULJUK

Reid and co-workers discovered similar speciation in an investigation of the coordination chemistry of germanium chlorides with sulfur-containing crown ethers such as [15]ane-S_2O_3 and [18]ane-S_3O_3. Both of the salts obtained from the reaction of $GeCl_2$·dioxane with the polyether are of the general form [GeCl(ane)][$GeCl_3$] (ILIHAN, ILIHER, ILIHIV).[141] Only the mono triflate salt [GeCl([18]ane-S_3O_3)][OTf] was obtained when reaction was done in the presence of excess Me_3SiOTf ; the apparent relative inertness of ligated Ge–Cl^+ ions to substitution has been observed regularly in such systems so the order of reagent addition is often critical – desired ion exchange reactions may need to be done prior to the addition of the binding ligand. Perhaps not surprisingly, the cations in each of the [18]ane-S_3O_3 salts feature an umbrella-like geometry similar to those observed for the all-oxygen analogues but the arrangement of the polyether appears to be influenced by the position of the heavier chalcogen atoms. Specifically, in each cation, the germanium atom is bound (in a *mer*-like manner) at the oxygen-containing half of the ligand and only the two sulfur atoms that are vicinal to oxygen engage in chelation (Figure 43, ILIHAN). The remaining sulfur atoms in these complexes engage in secondary bonding interactions with adjacent ions. For the complex with the smaller [15]ane-S_2O_3 ligand (ILIHIV), the cation contains a polyether with a folded arrangement reminiscent of the crown ether structure

[GeCl([15]crown-5)]$^+$ described above. Within the [GeCl([15]ane-S_2O_3)]$^+$ cation (Figure 44, ILIHIV), it is the sulfur-containing portion of the ligand that binds the germanium atom. The authors noted that, in all cases, the geometry about the germanium atom is consistent with the presence of a stereochemically-active pair of non-bonding electrons and they attributed the differences in binding modes to different physical and geometrical constraints of the ligands. The authors also reported the structures of some analogous poly-seleno-ether complexes ([8]ane-Se_2, [16]ane-Se_4, [24]ane-Se_6) in this work but all of the mixtures produced coordination polymer networks composed exclusively of carbenic GeX_2 fragments coordinated in an exocyclic fashion by the cyclic polydentate donor. In fact, it is important to note that the presence of multiple oxygen atoms in such polydentate donors appears to critical because similar reactions using polythioethers (e.g. [18]ane-S_6) or their heavier congeners only yield exocyclic binding of neutral GeX_2 units (Figure 45, ILIGUG) and do not generally result the ionic speciation that is typical of the crown ether complexes.[142-145]

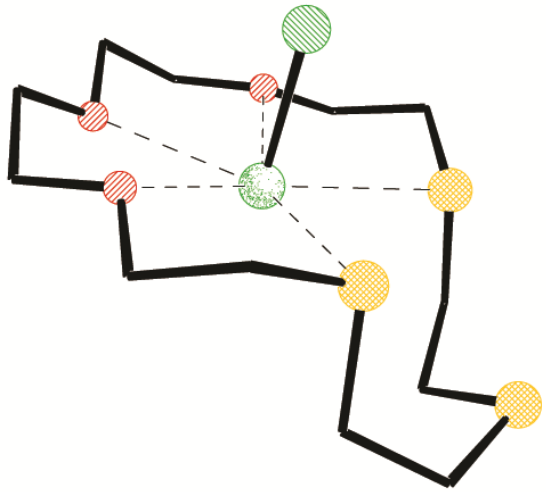

Figure 43. [GeCl([18]ane-S_3O_3)]$^+$ – ILIHAN

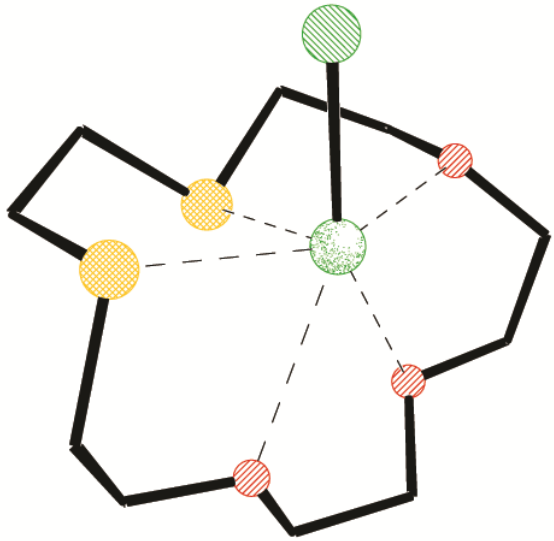

Figure 44. $[GeCl([15]ane\text{-}S_2O_3)]^+$ – ILIHIV

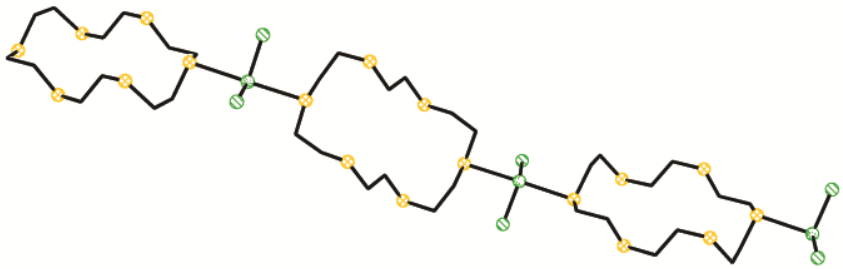

Figure 45. $[GeCl_2([18]aneS_6)]$ – ILIGUG, the $[18]aneS_6$ and the $GeCl_2$ fragments form infinite chains as shown in the picture. There is also an interaction between the chlorides of one chain with the germanium atoms of a parallel chain forming cross-linked network.

In terms of further chemistry of germanium(II) crown ether complexes, Macdonald and co-workers reasoned that the more open arrangement of the salt $[Ge([15]crown\text{-}5)][OTf]_2$ in comparison to the encapsulated Ge^{2+} ions in the crypt[2.2.2] and *bis*-[12]crown-4 sandwich salts might render it more accessible to other reagents. They found that the treatment of $[Ge([15]crown\text{-}5)][OTf]_2$ with one equivalent of water (or D_2O) generates the adduct $[Ge(OH_2)([15]crown\text{-}5)][OTf]_2$, Figure 46 (FIBSOA and FIBSOA01), in quantitative yield.[146] In the solid state, the adduct features a water molecule that is

hydrogen-bonded to two adjacent trilflate anions and that has an O···Ge distance of 2.003(4) Å. NMR experiments demonstrated that the adduct is in rapid equilibrium with the component species in solution and reactions with a variety of bases indicate that coordination of water to Ge^{2+} makes it a stronger Brønsted-Lowry acid. The authors postulated that the adduct could be considered as a diprotonated form of germanium monoxide and mass spectrometric and solution NMR data were indicative of the formation of [Ge(OH)([15]crown-5)][OTf] upon treatment with base. An analogous compound is formed when $[Ge([15]crown-5)][OTf]_2$ is treated with one equivalent of ammonia and pXRD investigations indicate that the resultant $[Ge(NH_3)([15]crown-5)][OTf]_2$ complex is isostructural with the water adduct. The nature of the bonding in these compounds was elucidated by DFT calculations in conjunction with NBO and AIM analyses. The bonds in the singly deprotonated models were found to be considerably stronger – and more covalent by Haaland's definition[147] – than those in the parent adducts. [146]

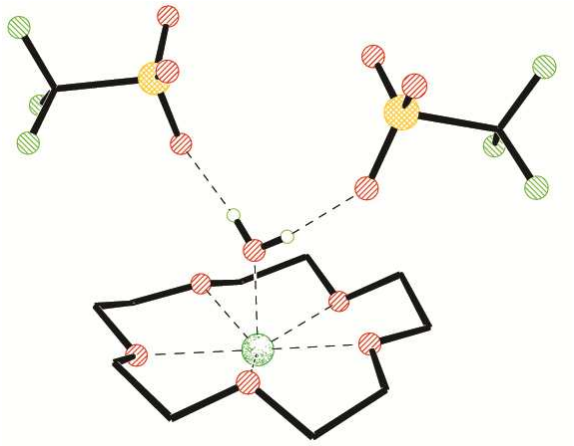

Figure 46. $[Ge(H_2O)([15]crown-5)][OTf]_2$ – FIBSOA01

The complexes reported by Sarazin and co-workers (ODIMEV, ODIMIZ, ODIMOF)[124, 125], along with analogous species containing tin(II) and lead(II), feature aza-polyether fragments of the form [12]ane-O_3N or [15]ane-O_4N in which the germanium(II) centers are held in close proximity to the amine

by the aryloxymethylene bridges (Scheme 12). [148] All of these low valent group 14 complexes, in addition to non-polyether-containing analogues, were investigated as catalysts for the immortal ring opening polymerization (iROP)[148] of lactide however the crown ether functionality was used primarily bind lithium ions in order to generate bi-metallic catalyst precursors rather to interact directly with the group 14 element.

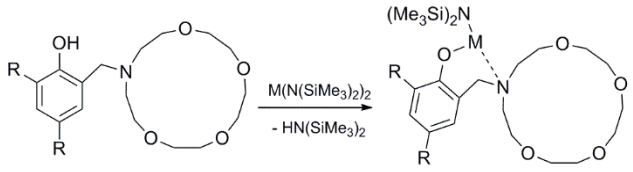

Scheme 12. [12]ane-O_3N (**21-H**) treatment with M(II) (M = Ge, Sn, Pb) and the resulting product which shows the metal interaction with the amine.

2.3.2 Germanium(IV)

At present there are no structurally characterized polyether complexes of germanium(IV).

2.4 Silicon

As of writing, there is only a single example of a crown ether complex of silicon and it is a relatively unstable complex of silicon(II).

Jutzi and coworkers reported that the reaction of the remarkable silicon(II) salt $[Cp^*Si][B(C_6F_5)_4]$[149] with DME or [12]crown-4 generates highly air- and moisture-sensitive 1:1 complexes which are thermally labile.[150] The structure of the cation $[Cp^*Si([12]crown-4)]^+$ (UVUYEQ) may be described as “sandwich-like” and features long Si···O distances of 2.8200(12)-3.0588(12) Å. MP2

calculations on related model compounds indicated that the nature of the Si···O bonds in these complexes is primarily electrostatic and van der Waals in nature. The particular mode of decomposition exhibited by these complexes suggested a potential application to the authors: they discovered that the $[Cp^*Si]^+$ cation causes the degradation of the polyether ligand to which it is bound. For example, the [12]crown-4 ligand is decomposed into 1,4-dioxane molecules, and acyclic polyethers of the general form $RO(CH_2CH_2O)R'$ are decomposed into 1,4-dioxane and all of the possible acyclic ethers (ROR, ROR', R'OR'). Further experiments demonstrated that the degradation reaction can be accomplished in a catalytic manner using salts of the $[Cp^*Si]^+$ cation.

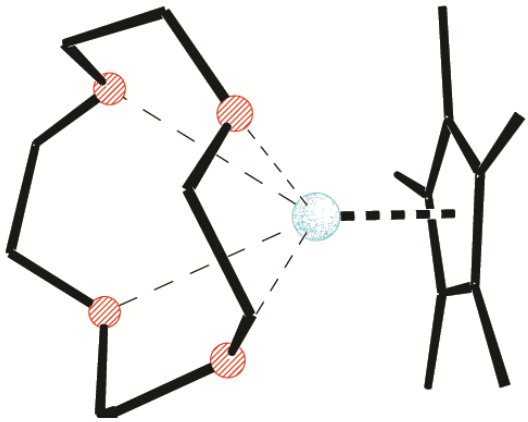

Figure 47. $[Cp^*Si([12]crown-4)]^+$ (UVUYEQ)

3. Group 13

The presence of the additional electron density associated with a low-valent element usually alters significantly the chemistry of the compounds containing that electron-rich center.[27, 151] For group

13 – in contrast to the typical Lewis acidity that is characteristic of triel(III) compounds – compounds containing triel(I) centers have the potential to behave as either Lewis acids or as Lewis bases.[152] As also highlighted for group 14, periodic trends render lower oxidation states more favorable for the heavier elements in the group such that thallium(I) is usually the most stable oxidation state for ions of that element.[147] Although indium(III) compounds are usually more stable than indium(I) analogues, both oxidations states have comparable stabilities and many compounds of each are known. For the lighter elements, the +3 oxidation state is much more stable, particularly in the case of aluminum. Perhaps as a consequence of the foregoing, the distribution of structurally characterized complexes of the elements with polyether ligands is dominated by complexes of thallium(I) (54 of 101 total CSD records for group 13); however, because all of the heavier group elements are metallic, the trend is not as clear as that observed for group 14. Thus there are 22 CSD records for indium – 8 of which feature indium(III) fragments – and 22 records for aluminum – all of which contain aluminum(III). There are a total of five reported polyether complexes of gallium and only three of these features gallium(I).

3.1 Thallium

The vast majority of polyether complexes of thallium contain thallium(I). In many instances thallium(I) (either with or without the polyether ligands) was selected as a counter cation for *anions* of interest in order to take advantage of the synthetic convenience and for the solubility properties engendered by the ion. Although such compounds have many practical applications, particularly for synthetic chemistry, they are not examined explicitly in this review.[153]

3.1.1 Thallium(I)

As noted above, in contrast to the remainder of group 13 elements, thallium shows preference for the +1 oxidation state over the +3 oxidation state. This is attributed to what is known as the "inert electron pair" effect which is a result of the relativistic effect on the 6s orbital.[154] The relative inactivity of this inert lone pair was long believed to be a result of ineffective s-p mixing that could be prerequisite for stereochemical activity.[154] Reiger and Mudring, however, illustrated via theoretical investigations that this is not always the case; rather, it is the minimization of antibonding orbital interactions of the lone pair orbital with its surrounding (filled orbitals in close proximity) that engenders the apparent stereochemical activity to the non-bonding pair of electrons. Figure 48 shows the structure of [Tl([18]crown-6)][ClO_4] (CAWCIN) in which the Tl^+ ion sits above the O_6 plane of the crown ether; this is in contrast to the structure observed for the potassium analogue in which the potassium ion sits at the centroid of the O_6 ring. The authors asserted that the observed structural distortion in the case of thallium(I) minimizes these repulsive antibonding interactions; the distortion from spherical symmetry of the orbital that had been primarily the Tl $6s^2$ electrons is responsible for the apparent manifestation of stereochemical activity.[154] Note that [Tl([18]crown-6)]$^+$ has been crystallographically characterized and reported with different anions, including: $[ClO_4]^-$ (CAWCIN)[154], $[TlI_4]^-$ (CAWCOT)[154], $[PF_6]^-$ (EMAPAJ)[155], $[CuBr_4]^-$/$[MnCl_4]^-$ (JUKXES01/HEWMOL)[156]

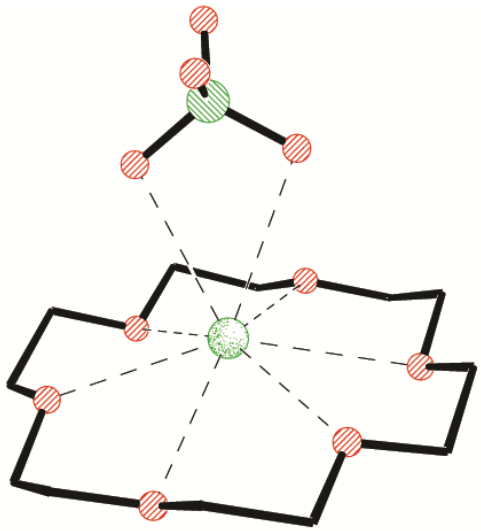

Figure 48. [Tl([18]crown-6)][ClO_4] – CAWCIN

Reiger and Mudring also prepared and structurally characterized the salt [Tl([18]crown-6)][TlI_4]·2H_2O (and the related hydronium and ammonium salts [H_3O([18]crown-6)][TlI_4]·2 H_2O, and [H_4N([18]crown-6)][TlI_4]·2H_2O, respectively) in order to demonstrate that the materials may indeed be crystallized in an *Fd-3* space group in the absence of a transition metal guest (although the presence of a catalytic amount of a transition metal halide appears to be required).[157] This result was noteworthy because the frameworks had initially been observed in supramolecular host-guest structures of the general type [$M^{II}X_4$][cat([18]crown-6)][TlX_4]·2 H_2O (M^{II} = Cu, Co, Zn, Mn; cat = Rb^+, NH_4^+, Tl^+; X = Cl, Br), but it was not clear if it was reasonable to consider the thallate framework as a host.[157]

In spite of the relatively minor distortions indicated above, it is well established that thallium(I) can mimic alkali metal ions such as potassium(I) (1.52 Å for K^+ vs 1.64 Å for Tl^+).[158] This behavior has many potential uses because, unlike potassium, thallium is NMR active and can allow for analysis of binding site studies using NMR spectroscopy.[159] For example, Alizadeh and co-workers studied the binding of thallium(I) to different polynuclear ligands.[28] They found that the treatment of 1,3-calix[4]bis-o-benzo-crown-6 with Tl[ClO_4] results in the thallium complex (**23**) shown in Figure 49 (NACQEP). ^1H NMR studies revealed that complexation of the Tl^+ results in a shift of the signals attributable to the methylene protons on the polyether to lower frequencies. The Δδ values (Δδ = $\delta_{complex}$ - $\delta_{free\ ligand}$) for the resulting complex reveal a very modest deshielding of the protons on the O–CH_2–CH_2–O fragment (Δδ ~ +0.05 ppm). This change in the spectrum is very small in comparison those observed for some other ligands (e.g. some calixarene ligands feature Δδ values of about –0.19 and +0.12 ppm for the bridging CH_2's). More reliably, identification of very different NMR signals for bound ^{203}Tl nuclei provides a direct method for the identification of complexed thallium(I) ions. For example, free thallium(I) species show a distinct signal at ca. –199 ppm whereas a signal is observed at –402 ppm upon formation of complex **23**.

An intermediate resonance at –364 ppm was attributed to a dithallium(I) complex observed at low concentrations of ligand added; the signal disappears upon the addition of sufficient ligand to form the monothallium(I) complex **23**. The rate of exchange for complex formation using the more rigid ligands is slow on the ^{203}Tl NMR timescale so signals for the free Tl^+ and the intermediate complex – or for the intermediate complex and the final complex **23** – are observed simultaneously, depending on the ligand concentration. Interestingly, when they performed similar experiments using a more flexible calixarene-crown ether ligand that features only a single crown ether fragment, they found that the exchange process is fast on the ^{203}Tl NMR timescale and only a single peak is observed.

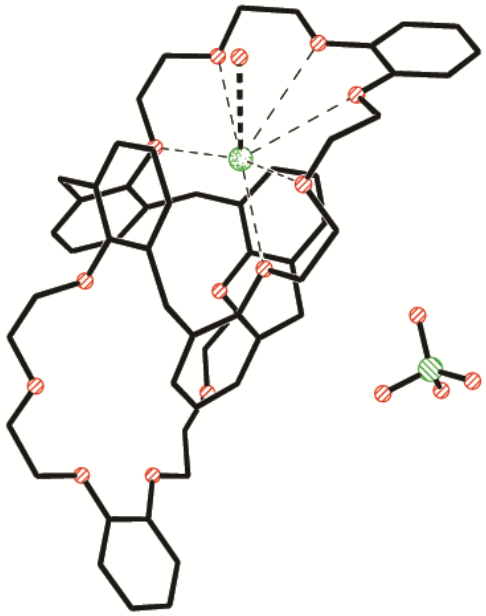

Figure 49. Compound **23** [(1,3-calix[4]bis-o-benzo-crown-6)Tl(H_2O)][ClO_4] – NACQEP; the hydrogen atoms on the water molecule were not present in the CSD record.

It is perhaps worth noting that the softness of thallium can have a significant effect on its chemical behavior. For example, during the investigation of some hybrid polyether calixarenes ligands that were initially designed for the selective separation of Cs^+ from other alkali metal ions, Talanova and co-workers discovered that calix[4]arene-bis(crown-6) have an even higher affinity for Tl^+. In fact, they

found that the extraction constant for Tl^+ is 10-fold greater than for Cs^+.[160] The authors demonstrated that thallium(I) has stronger tendency to π-coordinate with the aromatic rings of the calixarene system and they rationalized the increased preference for the triel monocation in that context.[160] After investigating calixarene systems and their coordination to thallium(I)[160], Talanova and co-workers synthesized a fluorogenic derivative of 1,3-*alternate* calix[4]arenebis(crown-6) (Figure 50) that was employed in the selective sensing of thallium(I) and cesium(I) at low concentrations.[161] As thallium(I) concentration is increased in a CH_3CN/H_2O solution of the ligand, fluorescence emission maximum shifts from 541 nm to 495 nm.

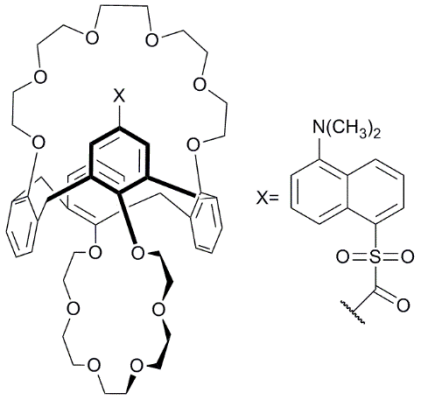

Figure 50. 1,3-*alternate* calix[4]arenebis(crown-6)

In a different vein, Pietschnig and co-workers investigated the complexation of different metal cations with m-terphenyl-substituted tetrafluorosilicates.[162] Although potassium(I) and thallium(I) share similar ionic radii and binding, treatment of $M[DMPSiF_4]$ (DMP = 2,6-dimesitylphenyl, M = K or Tl) with [18]crown-6 results in the compounds shown in Figures 51 (CUQJUU) and 52 (CUQKAB) respectively. The potassium complex features close F···K contacts between the cation and anion whereas the cation-anion interaction in the thallium analog is with the arene fragment of the ion. [162]

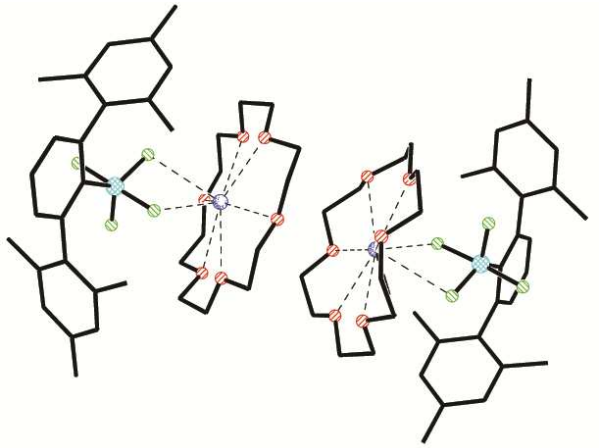

Figure 51. [K([18]crown-6)][DMPSiF$_4$] – CUQJUU

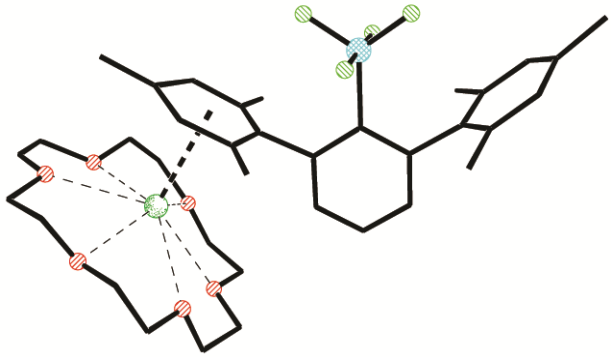

Figure 52. [Tl([18]crown-6)][DMPSiF$_4$] – CUQKAB

In an extensive investigation of the coordination chemistry of thallium(I) with in the presence of non-coordinating anions, Bochmann and co-workers reported that the treatment of [Tl(DME)][A] (where A = [$H_2N\{B(C_6F_5)_3\}_2$] with [18]crown-6 in CH_2Cl_2 results in a 1:2 thallium to ligand complex.[125] The identity of this complex was confirmed by NMR spectroscopy and microanalysis; however, upon recrystallization of the complex from a CH_2Cl_2/light petroleum mixture, a 1:1 complex (Figure 53, TEYLAL) is obtained instead as shown in Scheme 13. In this case, it is clear that the π-systems in these less-electron-rich arenes do not interact as effectively with the thallium(I) ions and interactions with the F atoms are observed instead.

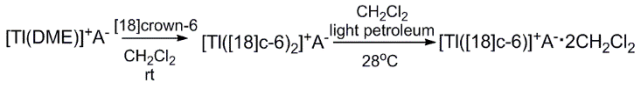

Scheme 13. Reaction scheme showing the synthesis of $[Tl([18]crown\text{-}6)][H_2N\{B(C_6F_5)_3)\}_2]\cdot 2CH_2Cl_2$ (TEYLAL).

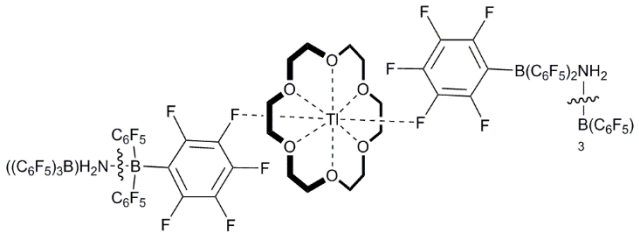

Figure 53. $[Tl([18]crown\text{-}6)][H_2N\{B(C_6F_5)_3\}_2]$. The structure is authenticated with scXRD (TEYLAL) but a chemical drawing is presented for clarity.

It should be noted that a structurally authenticated "sandwich" complex of Tl(I) has been known for a long time in the form of a *bis*([12]crown-4) complex $[Tl([12]crown\text{-}4)_2][SbCl_6]$ (LEBKIM), which features a "bent-sandwich arrangement".[163] Stability constant determinations reveal that a *bis*([15]crown-5) complex exists in propylene carbonate solution although no scXRD data have ever been reported.[164]

3.1.2 Thallium(III)

There have been no recent reports of thallium(III) crown ether complexes but several examples of complexes of the form $[TlX_2(L)][TlX_4]$ are known (L = [18]crown-6, DB[18]crown-6, DC[18]crown-6, and other [18]crown-6 variants) (ZEZFAL, XORQIE) as are several salts with $[TlMe_2(L)]^+$ ions featuring linear $TlMe_2^+$ cationic fragments (DUZBOP, DUGYIN, BUDHAJ, BEZNAV, BEZMUO).[165-168]

3.2 Indium

Although salts containing indium(I) are well known, the solubility of typical inorganic salts such as those of halides is very poor.[169] Attempts to solubilize such salts with donors usually results in rapid disproportionation and successful efforts in that regard remain rare.[170] The multiple coordination and weak binding of polyether ligands provides one approach that has yielded positive results in this regard and investigations into the species generated as part of such investigations have yielded many interesting insights into fundamental aspects of low valent chemistry.

3.2.1 Indium(I)

For organometallic compounds, the relative instability of the +1 oxidation state for indium has typically been overcome with through the design of ligands that provide adequate steric and or electronic stabilization of the univalent atom.[151] As indicated above, attempts to use coordination chemistry to isolate stable inorganic indium(I) compounds were generally unsuccessful and resulted in disproportionation to indium metal and higher oxidation state indium compounds. [171] Macdonald and co-workers postulated that indium(I) centers could be stabilized by using appropriately sized donors such as crown ethers because of their ability to occupy the complete torus of vacant orbitals on an indium(I) ion.[26] Andrews and Macdonald reported that the treatment of the soluble indium(I) reagent In[OTf][172] with [18]crown-6 resulted in the isolation of the product shown in Figure 54 (**24**, TAZFUW). The complex exhibits a structure in which the indium atom is bound in a *mer* conformation by the crown ether and features In···O_{crown} distances ranging from 2.8299(18) – 2.9292(18) Å and exists as a contact ion pair with an In···OTf distances of 2.370(2) Å. When analogous reactions were attempted using InCl, only products resulting from disproportionation (see below) were observed so it is apparent that the nature of the counter anion is of critical importance in the case of indium(I). The complexation of In[OTf] with the crown ether increases the solubility of the indium(I) salt considerably and appears to

prevent disproportionation in solvents such as THF, in which In[OTf] decomposes rapidly. Furthermore, the authors observed that whereas the free salt In[OTf] does not react at an appreciable rate with chlorocarbon solvents, the presence of [18]crown-6 causes the indium(I) center to undergo a rapid oxidative addition into the C–Cl bond, as illustrated in Scheme 14.[26] The generation of the resultant organo-indium(III) cation provides insight into the behavior of indium(I) reagents in important synthetic organic transformations (see the indium(III) section below).

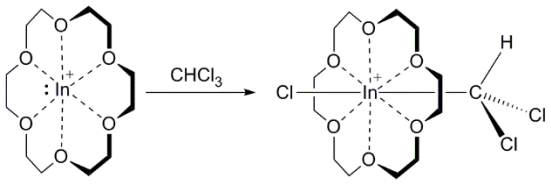

Scheme 14. Reactivity of [In([18]crown-6)][OTf] with $CHCl_3$.

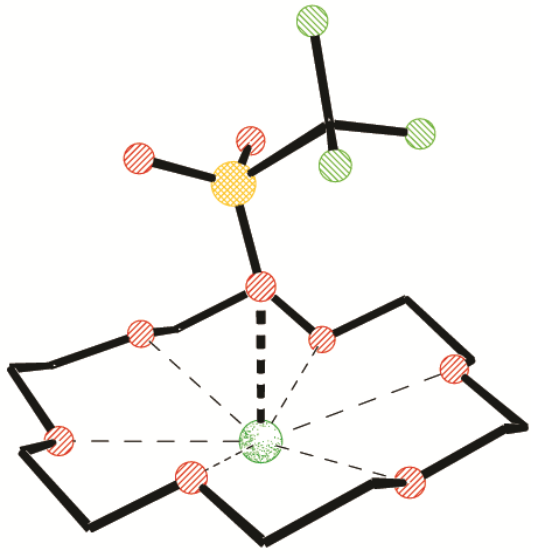

Figure 54. [In([18]crown-6)][OTf] – TAZFUW; complex **24**.

The same research group also showed that the treatment of In[OTf] with [15]crown-5 yields a complex with a sandwich structure $[In([15]crown\text{-}5)_2][OTf]$ (Figure 55, KOBRID)[173] that reminiscent of the isoelectronic tin(II) complexes.[118, 119, 122] They found that the sandwich structure is formed regardless of

the stoichiometry of [15]crown-5 employed in the reaction and that any excess In[OTf] remains unreacted. The centrosymmetric cation features a 10-coordinate environment about the indium(I) ion with In···O_{crown} distances ranging from 2.9082(12) – 3.0954(12) Å and there are no close contacts between In and the triflate anion. In contrast to the [18]crown-6 complex, [In([15]crown-5)$_2$][OTf] does not react with chlorinated hydrocarbon solvents.

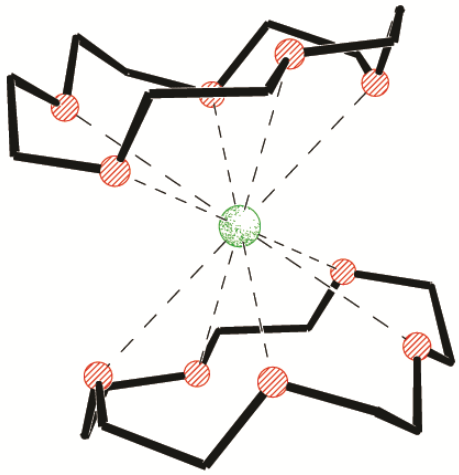

Figure 55. [In([15]crown-5)$_2$]$^+$ – KOBRID

Cooper and Macdonald subsequently reported that the treatment of [18]crown-6 with trifluoromethanesulfonic acid ([H][OTf]) generates the protonated crown ether salt [H[18]crown-6][OTf], which upon exposure to an In(I) source such as Cp*In[174] (or InCl) results in the protonolysis of Cp*H (or HCl) and the production of [In([18]crown-6)][OTf] in excellent yield.[175] The same protocol was employed using trifluoroacetic acid (HTFA) to generate the salt [In([18]crown-6)][TFA] (**25**) (Figure 56, PUVDEQ). Complex **25** has a structure very similar to that of the triflate analogue and features In···O_{crown} distances ranging from 2.785(5) – 2.985(5) Å and is also best considered as a contact ion pair with a short In···O_{TFA} distance of 2.272(5) Å. The success of this synthetic approach was particularly noteworthy because the free salt "In[TFA]" is very unstable under the conditions used and rapidly disproportionates whereas the "crowned" variant of the salt appears to be stable indefinitely. The use of protonated polyethers holds

great promise for the preparation and isolation of similarly "unstable" species.[175] Another important observation made in this work was that the reaction of [H[18]crown-6][OTf] with indium metal generates [In([18]crown-6)][OTf] in good yield with the elimination of H_2. Such a result is important in that it provides a simple approach for the direct generation of an indium(I) reagent starting from the metal.

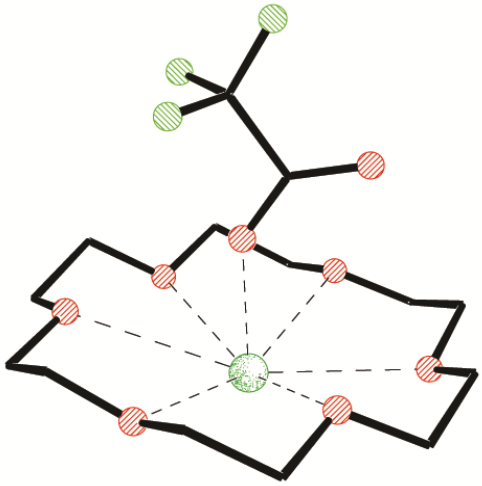

Figure 56. [In([18]crown-6)][TFA] – PUVDEQ

Macdonald and co-workers investigated the reactivity of **24** ([In([18]crown-6)][OTf]; Figure 54) with different group 13 Lewis acids such as $InCl_3$, $InBr_3$ and InI_3.[176] In each case, the reaction resulted in the replacement of triflate anion with a halide anion and the coordination of the resultant In(I) halide donor to the indium trihalide acceptor to yield complexes of the type [InX([18]crown-6)→InX_3], as illustrated in Scheme 15 and figure 57 (TAZGEH, UWATUI, UWAVAQ, UWAVEU, UWAVIY, UWAVOE). Identical complexes were also obtained from the reaction [18]crown-6 variants with InX and with "$InCl_2$". The In–In bond distances (X = Cl, 2.6727(7) – 2.6819(5) Å; X = Br, 2.7073(4) Å; X = I, 2.725(2) Å) increased as the halogen size increased, which is consistent with the decreasing Lewis acidity of the InX_3 as X is altered from Cl to Br to I.[176] The complexes feature nearly linear X-In-In fragments with angles

ranging from 170.09(4)-179.63(10)° and unique In^{I}-X distances (X = Cl, 2.3149(18) – 2.3334(9) Å; X = Br, 2.4572(5) Å; X = I, 2.663(3) Å). One indium ion lies roughly at the centroid of each crown ether and the range of In···O_{crown} distances in these complexes (2.481(5) – 3.081(5) Å) is consistent with those observed for the indium(I) complexes presented above. It should be noted that these donor-acceptor complexes represented a new valence isomeric form of "triel(II) halides": compounds containing the general formula M_2X_4 were known to exist as either as mixed valent salts[177] of the type $M^{I}[M^{III}X_4]$ or as species with element-element bonds of the type X_2M^{II}-$M^{II}X_2$, depending on the properties of any donors present but [18]crown-6 favors the form $XM^{I}\rightarrow M^{III}X_3$. As noted in the introduction, an alternative description of these complexes could be as zwitterionic indium(II) species $XIn^{II(+)}$-$In^{II(-)}X_3$ but DFT investigations reveal that heterolytic cleavage of the In-In bond is energetically favored, which is most consistent with the donor-acceptor description.

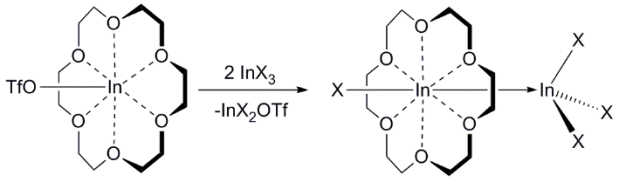

Scheme 15. Reactivity of [In([18]crown-6)][OTf] with InX_3 to produce [InX([18]crown-6)→InX_3].

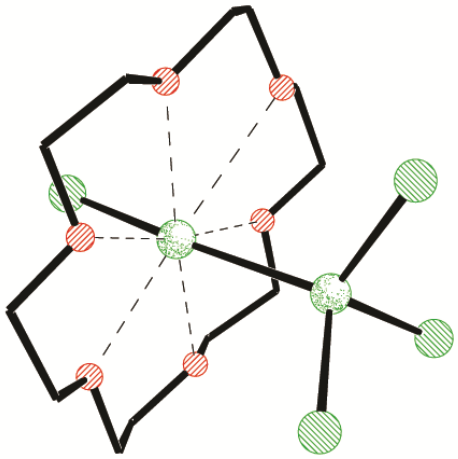

Figure 57. [InCl([18]crown-6)→$InCl_3$] – UWAVEU

In the same work, the researchers demonstrated that the donor-acceptor form is only observed in the solid state when the triel atom in the acceptor is indium. For example, when the reagent [In][ECl_4] (E = Al, Ga or In) is treated with [18]crown-6, complexes of the form [In([18]crown-6)][ECl_4] are obtained as shown in Scheme 16. Solution-phase ^{115}In, ^{71}Ga and ^{27}Al NMR investigations demonstrate that each of the compounds exists in the ionic form in MeCN solution and solid-state NMR investigations indicated that the aluminate and gallate salts [In([18]crown-6)][ECl_4] (E = Al, Ga) are present in the solid. The structure of the related gallate salt [In([18]crown-6)][$Cl_3Ga(OH)GaCl_3$] (UWAWEV) is illustrated in Figure 58 (left). Furthermore, when smaller crown ethers were used, only ionic species were observed; for [15]crown-5, these featured "sunrise" complexes such as the one illustrated for [In([15]crown-5)][$GaCl_4$] (UWAWAR) in Figure 58 (right) with In···O_{crown} distances of 2.608(3) – 2.777(3) Å. Several of these well-characterized materials were subsequently used for a comprehensive solid state ^{115}In NMR investigation of indium(I) species that demonstrated the utility of ^{115}In NMR for the study of structure and dynamics.[178] Of particular note is the considerable motion associated with the crown ethers (and some of the complexes) at room temperature in the solid state. More generally, the insights into the interpretation of spectral features is anticipated to be particularly for the structural analysis of important indium-containing materials that are not amenable to other forms of characterization.

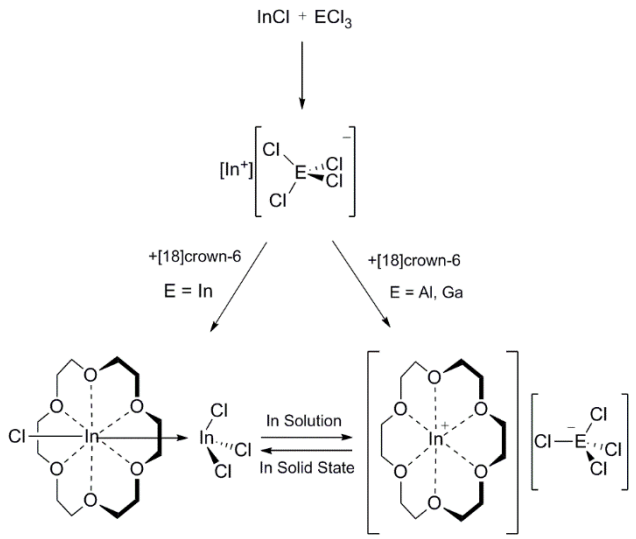

Scheme 16. Structural alternatives for [In([18]crown-6)][ECl_4] complexes.

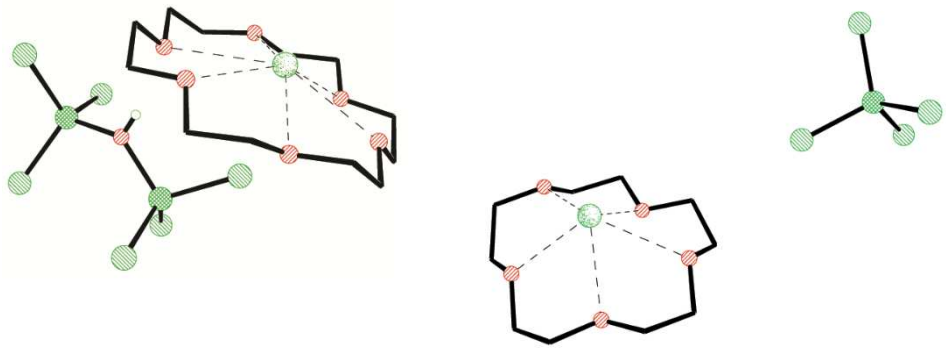

Figure 58. [In([18]crown-6)][$Cl_3Ga(OH)GaCl_3$] – UWAWEV (left), [In([15]crown-5)][$GaCl_4$] – UWAWAR (right).

Cooper and Macdonald demonstrated that is it possible to displace the indium(I) ion from [18]crown-6 with a potassium ion.[179] For example, the treatment of solutions of the very soluble [In([18]crown-6)][OTf] complex with KX (X = Cl, Br, I), results in the immediate formation of finely dispersed powders of InX. Such finely dispersed indium(I) halides may have practical applications in synthetic applications given the insolubility and instability of the bulk indium(I) halide salts.

Krossing and co-workers reported that the treatment of $[In][Al(OCCF_3)_3)_4]$ with [18]crown-6 in PhF results in the formation of the complex $[In([18]crown\text{-}6)(PhF)_2][Al(OCCF_3)_3)_4]$ depicted in Figure 59 (ZEGNAC).[180] The signal in the solution ^{115}In NMR spectrum for the starting fluorobenzene complex of In^+ at −1335 ppm is replaced by a signal at −1094 ppm which is indicative of complex formation. As in several of the cations presented above, the [18]crown-6 is belted around the indium(I) ion in a *mer* fashion with $In\cdots O_{crown}$ distances of 2.761 – 2.943 Å; the average distance of 2.841 Å is marginally shorter (by 0.03 – 0.08 Å) than the averages distances observed in [In([18]crown-6)][OTf] and [In([18]crown-6)]$[Cl_3Ga(OH)GaCl_3]$. The shorter distances are likely a consequence of the much less coordinating nature of $[Al(OCCF_3)_3)_4]^-$ anion,[181, 182] which results in the absence of close cation-anion interactions. Rather than interacting with the anion, the indium(I) ion interacts instead with two fluorobenzene molecules. In the solid state structure, one of the PhF molecules is bound in a η^6-fashion with an In···centroid distance of 3.26 Å while the other forms an η^1-complex with an In···C distance of 3.50 Å. Similar structural features were observed for the gallium(I) analogue (see below) and, on the basis of DFT investigations, the authors postulated that the differences observed in the arene interactions may be a manifestation of a stereochemically active lone pair of electrons on the triel(I) ion.

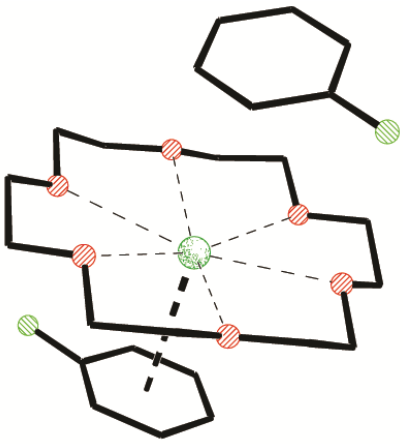

Figure 59. $[In([18]crown\text{-}6)(PhF)_2]^+$ – ZEGNAC

3.2.2 Indium(III)

As described in the preceding section, some crown ether complexes of indium(I), such as [In([18]crown-6)][OTf], undergo formal oxidative addition reactions to generate indium(III) species.[26] Furthermore, a handful of other polyether complexes have been observed resulting from reactions with indium trihalides[176] and even trimethylindium[183]. For example, the treatment of [In([18]crown-6)][OTf] with either $CHCl_3$ and CH_2Cl_2 results in the formal insertion of the indium(I) center into a C–Cl bond although the mechanism through which this process occurs was not elucidated. Figure 60 shows the products resulting from the reactions of [In([18]crown-6)][OTf] and [In(DB[18]crown-6)][OTf] with $CHCl_3$.[26, 184] The cation from the resultant salt [Cl–In–$CHCl_2$([18]crown-6)][OTf] (ODUWIU) exhibits a structure in which 5 of the ligand's oxygen atoms are arranged in a *mer* arrangement about the indium(III) ion – the In···O_{crown} distances range from 2.409(9)-2.531(8) Å and are considerably shorter than those found in the starting indium(I) complex – and the remaining O atom engages in hydrogen bonding with the methine proton derived from the chloroform. In contrast, the analogous salt [Cl–In–$CHCl_2$(DB[18]crown-6)][OTf] (TAZGAD) derived from the more rigid benzannulated ligand features considerably longer In···O distances (2.517(5)-2.756(5) Å) consistent with the constraints of the polyether. As indicated above, it is noteworthy that the insertion reaction does not occur at an appreciable rate for the non-ligated salt [In][OTf], which illustrates the potential activating power afforded by complexation with the polyether. The use of low-valent indium reagents in organic chemistry is extensive[72, 73] and the complexes described herein can be considered as providing models of the proposed intermediate species that have been trapped by the crown ethers.

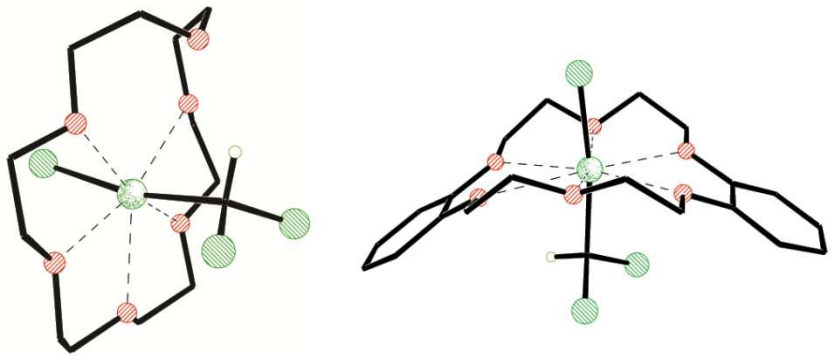

Figure 60. $[Cl–In–CHCl_2([18]crown-6)]^+$ – ODUWIU (left), $[Cl–In–CHCl_2(DB[18]crown-6)]^+$ – TAZGAD (right).

In contrast to donor-acceptor complexes obtained from the reaction of [In([18]crown-6)][OTf] with indium trihalides, the treatment of [In([18]crown-6)][OTf] with trimethylindium results in disproportionation. One of the products that is consistently crystallized from that reaction is the salt $[Me_2In([18]crown-6)][OTf]$ (IJOTEH) depicted in Figure 61.[183] The cation features a linear $InMe_2^+$ fragment that is bound by the *mer* conformation by the crown ether. The $In\cdots O_{crown}$ distances range from 2.620(2) – 2.842(2) Å.

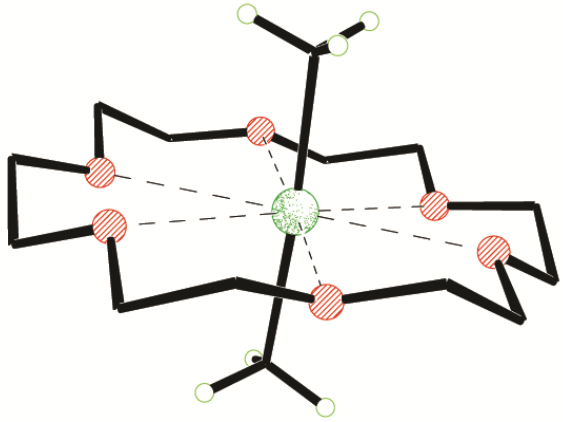

Figure 61. $[Me_2In([18]crown-6)]^+$ – IJOTEH

In contrast to the C-Cl insertion reactions outlined above, Macdonald and coworkers had found that the reaction of [In([18]crown-6)][OTf] with CCl_4 results in the generation of salts containing $[InCl_2([18]crown\text{-}6)]^+$ ions on the basis of mass spectrometric data. No structural data was presented however Krossing and co-workers reported the structure of the salt $[Cl_2In([18]crown\text{-}6)][Al(OC(CF_3)_3)_4]$ (GEQHIV) in a private communication to the CSD. The cation of this salt is depicted in Figure 62 and, as in the structure ODUWIU, the [18]crown-6 ligand adopts a geometry in which five of the oxygen atoms bind the indium(III) ion closely with $In\cdots O_{crown}$ distances from 2.289-2.350 Å and the remaining oxygen atom does not appear to interact with the metal. The $InCl_2$ fragment is essentially linear with an angle of 177.35° and the In-Cl distances are 2.353 and 2.358 Å.

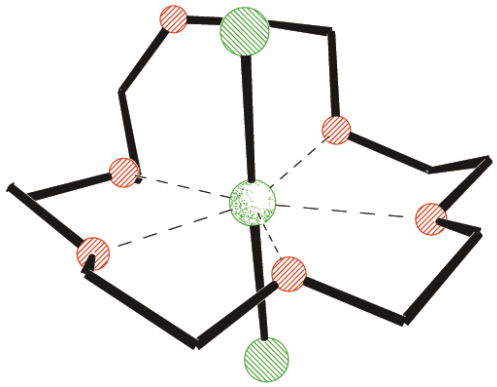

Figure 62. $[Cl_2In([18]crown\text{-}6)]^+$ (counter ion, $[Al(OC(CF_3)_3)_4]$, omitted for clarity) – GEQHIV

A noteworthy older example of an indium(III) complex is $[InI_2(DB[24]crown\text{-}8)(H_2O)][InI_4]$ (Figure 63, WIYFEP) that was reported by Willey and co-workers that was obtained from the treatment of DB[24]crown-8 with InI_3 in acetonitrile.[185] The large cavity crown ether had been used for the simultaneous entrapment of two identical alkali metal cations (Na^+ and K^+)[185] but the authors discovered that in the case of indium(III) cations, simultaneous entrapment does not occur. They found that a single indium(III) cation is bound and a water molecule occupies the fifth equatorial site to provide a roughly pentagonal bipyramidal geometry at indium. Although the position of the hydrogen atoms on

the entrapped water molecule were not identified in the crystal structure, the features of the molecule and FTIR data suggest that they are almost certainly engaged in hydrogen bonding interactions with oxygen atoms in the crown ether. Overall, the compound illustrates the possibility of using larger crown ethers to trap or stabilize larger ions or potentially reactive intermediates that may be of interest.

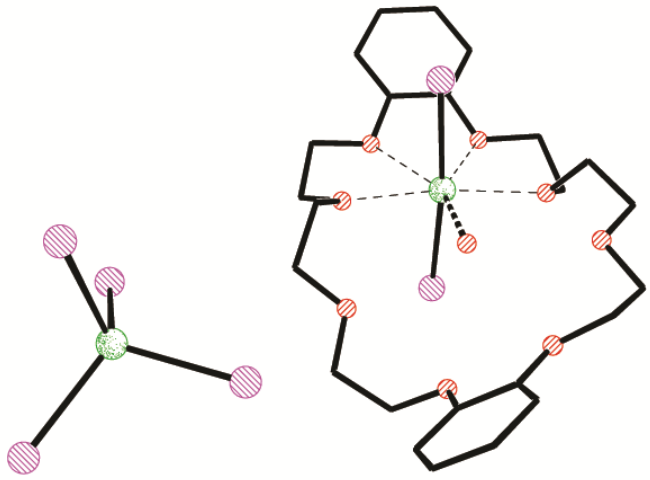

Figure 63. $[InI_2(DB[24]crown\text{-}8)(H_2O)][InI_4]$ – WIYFEP; hydrogen atom positions for the water were not in the CSD record.

3.3 Gallium

3.3.1 Gallium(I)

As indicated above, Krossing and co-workers were able to isolate a gallium(I) polyether complex analogous to the indium(I) complex described above.[180] They found that treatment of $[Ga][Al(OC(CF_3)_3)_4]$[186] with [18]crown-6 in PhF results in the formation of $[Ga[18]crown\text{-}6(PhF)_2][Al(OC(CF_3)_3)_4]$[180] (Figure 64, ZEGNEG). Evidence for complexation in solution was provided by the change in the chemical shift observed in the ^{71}Ga NMR spectrum: whereas the

gallium(I) starting material resonates at -756 ppm, the signal is observed at -643 ppm upon treatment with [18]crown-6. The crystal structure of the gallium(I) complex is isomorphous with that of the indium(I) analogue and also contains two solvent molecules coordinated to the metal center. The Ga···O_{crown} distances range from 2.665 – 2.895 Å with an average of 2.798 Å, which is shorter than the average In···O_{crown} distance of 2.841 Å in the heavier congener. Again, one of the molecules is bound in an η^6-manner with an In···centroid distance of 3.18 Å while the other exists as an η^1-complex with an In···C distance of 3.31 Å.[180] Taken together, these results suggest that the effective ionic radius of Ga^+ is roughly 0.2-0.4 Å smaller than that of In^+. As of writing, this compound is the only example of a mononuclear gallium(I) center coordinated to a polyether ligand reported in the CSD.

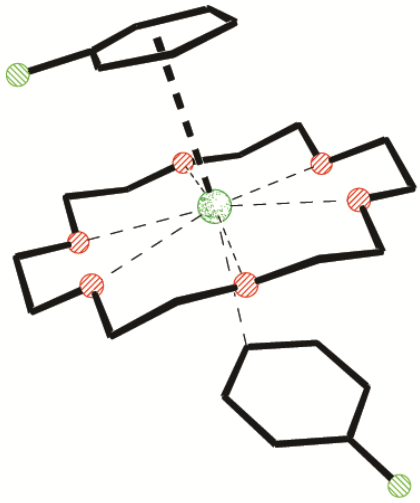

Figure 64. $[(Ga[18]crown\text{-}6)(PhF)_2]^+$ – ZEGNEG

Baines[187] and co-workers very recently reported the isolation of bimetallic gallium(I) cryptand[2.2.2] complexes. They found that the treatment of $Ga_2Cl_4(thf)_2$ with cryptand[2.2.2] in thf produces an off-white precipitate over time that was characterized as $[Ga_3Cl_4(crypt[2.2.2])][GaCl_4]$ (Figure 65, left, MUPDUY). Running the same reaction in toluene, but in the presence of excess Me_3SiOTf (TMS-OTf) results in the immediate formation of $[Ga_2Cl_2(crypt[2.2.2])][OTf]_2$ as a white

precipitate (Figure 65, right, MUPFEK). These two compounds represent the first examples of crypt[2.2.2] complexes that encapsulate two metals simultaneously and they are the first gallium(I) cryptand complexes reported. In the cation $[Ga_3Cl_4(crypt[2.2.2])]^+$, the Ga-Ga distance of the two encapsulated metals (2.4087(5) Å) is significantly shorter that the Ga-Ga distance to the external $GaCl_3$ fragment (2.4232(5) Å) and the Ga-Ga distance of 2.3812(4) Å in the dication $[Ga_2Cl_2(crypt[2.2.2])]^{2+}$ is considerably shorter. The authors used DFT calculations to conclude that, in both complexes, the encapsulated gallium centers are best treated as gallium(I) – the gallium atom in the $GaCl_3$ fragment is gallium(III) – and that the bonding between the gallium atoms is probably covalent in nature. As indicated earlier for the heavier group 13 elements, the redistribution of the chloride anions among the gallium atoms available is typical of mixed valent triel halide compounds.[177] More generally, the isolation of unusual and reactive bimetallic fragments within the polyether ligands highlights one potential area for future investigation and development.

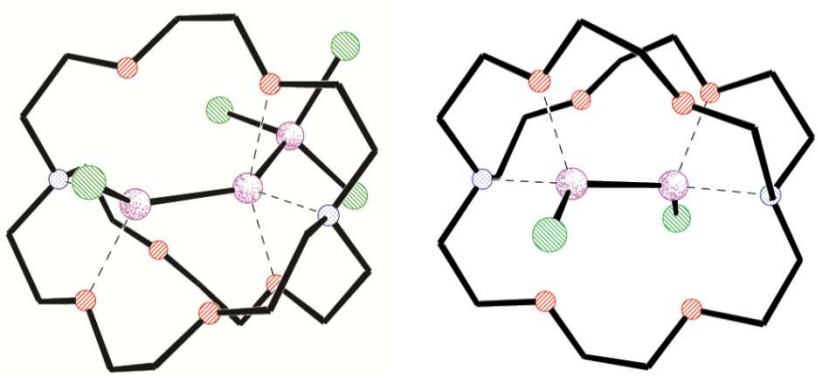

Figure 65. The cations from $[Ga_3Cl_4(crypt[2.2.2])][GaCl_4]$ (left, MUPDUY); $[Ga_2Cl_2(crypt[2.2.2])][OTf]_2$ (right, MUPFEK).

3.3.2 Gallium(III)

There have been no recent reports of gallium(III) complexes coordinated by polyether ligands but the only two structures every reported are illustrated here in Figures 66 and 67. The reaction of

$GaMe_3$ with DB[18]crown-6 produces the adduct [$(GaMe_3)_2$DB[18]crown-6] (VADTEZ) in which the two most basic oxygen atoms of the dibenzo(crown) ether engage in exocyclic donor-acceptor interactions with $GaMe_3$ in exactly the fashion that one would anticipate.[188] The structure obtained from the reaction of the aza crown ether ((NH,NH'-[18]ane-N_2O_4)) with trimethylgallium also features two $GaMe_3$ fragments that are bound in an exocyclic manner to the polyether portion of the ligand but it also includes a covalently bound $GaMe_2$ group that is endocyclic to the crown in $(GaMe_3)_2$·[$GaMe_2$(N,NH'-[18]ane-N_2O_4)] (JERLOH).[189] Whereas the coordination geometry about the gallium(III) atoms in each of the exocyclic $GaMe_3$ fragments is distorted tetrahedral, the additional oxygen atom ligation from the polyether affords a trigonal bipyramidal geometry for the endocyclic gallium(III) atom.

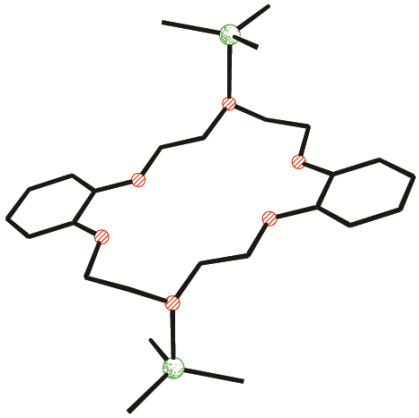

Figure 66. $(GaMe_3)_2$·O,O'-DB[18]crown-6 – VADTEZ[188]

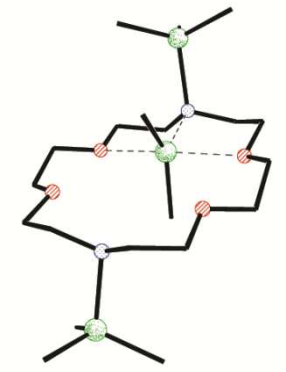

Figure 67. $(GaMe_3)_2 \cdot [GaMe_2(N,NH'\text{-}[18]ane\text{-}N_2O_4)]$ – JERLOH[189]

3.4 Aluminum

3.4.1 Aluminum(I)

No adducts of aluminum(I) with crown ethers or related ligands have ever been structurally authenticated. This is likely a consequence of the high reactivity of aluminum(I) in conjunction with the oxophilicity of aluminum.

3.4.2 Aluminum(III)

Although there have been no crystallographic structures reported for Al(III) complexes of crown ethers since 2000, there has been one report that uses a modified quinoline ester (PQTEG) as a colorimetric sensor for binding of aluminum which is monitored by UV-Vis and further confirmed by NMR and IR studies.[190] Treatment of PQTEG with aluminum(III) perchlorate in a mixture of acetonitrile/water (95:5; v/v) results in a color change from colorless to deep yellow (Scheme 17). PQTEG exhibits a strong absorption band at 254 nm and two weaker bands at 308 and 348 nm. In the presence of aluminium(III), the absorption bands of PQTEG are red shifted to 269, 332 and 415 respectively. As a consequence of the flexibility of the polyether molecule, the binding of a metal ion allows for a significant change in the ^{1}H NMR spectrum – again, this is a useful feature that is not often observed in fixed or rigid crown ethers. The protons around the quinolone underwent the largest change in chemical shift. Each of the signals for the protons in the complex are deshielded with respect to the free ligand and the changes in the shifts range from +0.2 and +0.8 ppm.

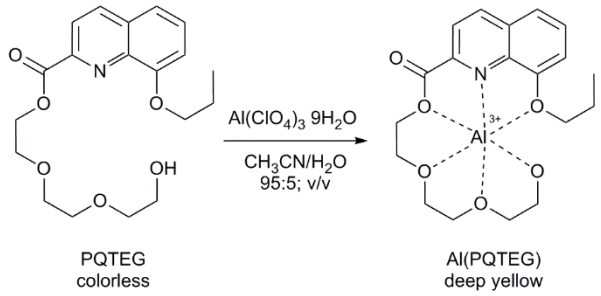

Scheme 17. Reaction of PQTEG with aluminum(III) perchlorate.

Some of the prior reports (prior to 2000) on Al(III) complexes of crown ethers are worthy of mention, primarily the work by Atwood and co-workers. The majority of the roughly two dozen structures reported previously are donor-acceptor complexes of the polyether with $AlMe_3$ (e.g. BOYVEQ) in which the metal(s) acceptors are situated external to the cyclic-ether and are bound to a single O atom. From a very broad perspective, these investigations were conducted in order to elucidate the behavior of $AlMe_3$ because of its importance and use a co-catalyst in olefin polymerization. Interestingly, when aluminum halides or organoaluminum halides were treated with related crown ether ligands, the resultant species were usually ionic salts in which the $[AlX_2]^+$ or $[AlR_2]^+$ cations are chelated by the ether. In these instances, both linear (*transoid*) and bent (*cisoid*) geometries about the aluminum atom were observed and the geometry of the cationic fragment appeared to be determined by the geometrical constraints of the ligand. For example, the salt $[AlCl_2(B[15]crown-5)][AlCl_3Et]$ (CUPSOV) contains a nearly linear dichloroaluminum cation with a Cl-Al-Cl angle of ca. 169° that is bound in a *mer*-like manner by the relatively rigid polyether.[191] In contrast, bent $[AlCl_2]^+$ cationic fragments are found in the structures of $[AlCl_2([12]crown-4)][AlCl_3Et]$ (DOJVIH) and $[AlCl_2([18]crown-6)][AlCl_3Et]$ (DOJVON), that feature smaller, or more flexible ligands, respectively.[71]

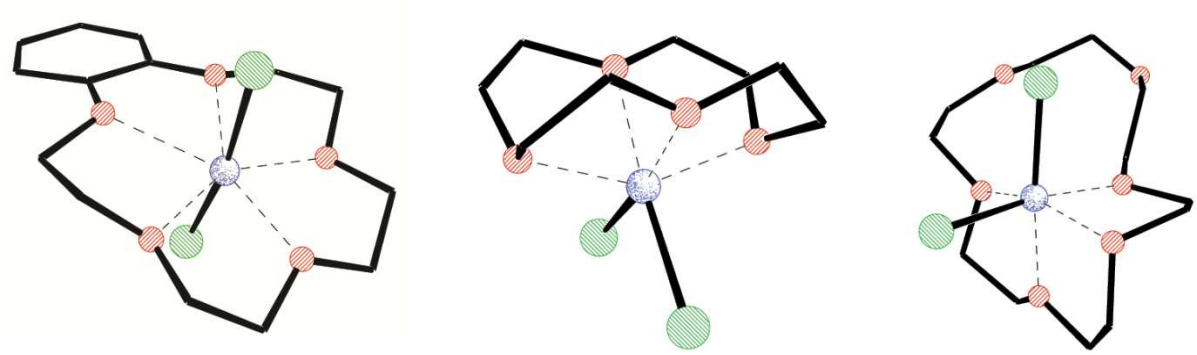

Figure 68. Left: $[AlCl_2(B[15]crown\text{-}5)]^+$ – CUPSOV; Center: $[AlCl_2([12]crown\text{-}4)]^+$ – DOJVIH; Left: $[AlCl_2([18]crown\text{-}6)]^+$ – DOJVON.

4. Conclusions and Outlook

There has been tremendous recent progress in the use of polyether ligands for the capture, detection, stabilization, or activation of heavier group 13 and 14 elements in the last decade. Although there are no endocyclic polyether complexes of boron or carbon – and the properties of "free" B^+ or C^{2+} ions render the challenge of doing so daunting – the development of reliable synthetic approaches to low valent p-block elements has allowed for the isolation of complexes containing even Si^{2+}, Ge^{2+} and Ga^+! Many useful polyether complexes have been reported and exploited for their chemical, physical, or material properties. From a fundamental standpoint, the increasing number of compounds known provides much insight into the chemistry of such complexes and into the difference in behavior observed for lower oxidation state analogs. As emphasized throughout this review, it appears as if the more metallic nature of lower oxidation state ions, particularly those in group 14, allows them to behave more like s-block elements and has provided for more endocyclic complexes of polyether ligands.

It was well-understood that polyether ligands featuring different sizes and levels of flexibility can be used to generate complexes of different stoichiometries and structures – this conclusion holds true

for the polyether complexes of the early p-block. Perhaps less obvious is the observation that, for many ns^2 systems, the use of a multitude of weak donors can result in stable compounds so long as the cation is coupled with appropriate counter anions. For indium(I), the identity and properties of the counter ions are also critical in determining if a complex will be stable. More generally, it is clear that interactions with counter anions in such systems often have a significant effect on the nature of the interaction between the polyether and the metal. In this context, the improvement of weakly coordination anion technology has allowed for significant advances in this area and may allow for the preparation of outstanding targets such as complexes of aluminum(I). Conversely, the controlled introduction of more strongly interacting counterions (or donors) may provide a convenient approach to activate the latent reactivity low valent complexes that have been stabilized using polyethers. We believe that investigations toward this end will yield many new and interesting transformations. Among these is the activation of small molecules as exemplified by the germanium(II) complex depicted in Figure 46, the silicon(II) complex presented in Figure 47, and in the indium complexes shown in Scheme 14, Figure 60 and Figure 63. Such complexes suggest potential avenues for small molecule activation and even C–H activation by other polyether triels and tetrels. Although the lighter analogs of group 13 and 14 polyether complexes are generally less stable, this renders them more reactive and potentially allows for a different kind of chemistry than that presented by the heavier analogs.

Heavier analogs of these polyether complexes have been known for a longer time as a consequence of the inherent stability of the lower oxidation state forms of the metals; such stability allowed for a more extensive development of applications and for the use of techniques such as MOCVD. The current development of stable lighter polyether complexes of triels and tetrels may allow researchers to use the well-established chemistry of elements such as lead and thallium as a model to guide future investigations. For but one example, it should be possible to develop new perovskite-like

materials with different physical properties (e.g. conductivity and resistance) that may allow for new kinds of applications or that could lead to an enhancement of existing applications.

In this vein, because of improvements in both computer power, software, and computational methodology, considerably more accurate DFT and post Hartree-Fock methods, in conjunction with sophisticated methods for analysis are now regularly applied to rationalize the bonding and reactivity of polyether complexes of even the heaviest p-block elements. Some of the analytical approaches that have proven very enlightening include: Atoms In Molecules (AIM), Natural Bond Orbital/Natural Population Analysis (NBO/NPA), Electron Localization Function/Electron Localization Index (ELF/ELI), among others. The use of such tools will surely increase in the future and will allow for the improved design of crown ether complexes that are tailored for a particular task.

The data presented in the preceding sections for complexes featuring relatively flexible polyether ligands allow one to make reasonable estimates as to the relative sizes of some of ions for which the ionic radii are missing from Table 1. For example, the mean In···O distance of ca. 2.87 Å from the metrical data from several unambiguous [18]crown-6 complexes of indium(I) suggest that the radius of In^{1+} is ca. 1.5 Å and very similar to that of K^{+}. Although there is only a single example for gallium(I), the mean value of the Ga···O distances of ca. 2.80 Å in the [18]crown-6 complex is consistent with a correspondingly smaller radius for Ga^{+} of ca. 1.4 Å. For the tetrel ions, the interesting behavior observed with [15]crown-5 ligands suggests that the S-P radius of 0.87 Å is reasonable for "free" Ge^{2+} ions but that germanium(II) ions in more covalently bound forms, such as $Ge\text{-}Cl^{+}$, must have a larger apparent radius of at least ca. 1.0 Å. Unfortunately, the unique example of a polyether complex with silicon(II) is a half-sandwich organometallic complex with properties that render such a simple analysis unreliable but the data for germanium(II) probably provides a reasonable upper boundary.

Finally, one should anticipate many new and interesting developments in the area of polyether complexes for the p-block elements. Continued development and use of such complexes in terms of sensing, detection, and sequestration applications is beyond question and the potential for applications involving crown-ether-based permanently porous liquids are particularly intriguing. Research and development of materials and materials precursors involving such species is also certain. In light of some of the more recent developments, it is also likely that major advances in small molecule activation and the trapping of reactive intermediates in appropriately designed polyether complexes will allow for stunning new observations in this area of modern main group chemistry.

5. Abbreviations

AIM = Atoms In Molecules

B = benzo

^{i}Bu = isobutyl

^{n}Bu = n-buyl

^{t}Bu = tert-butyl

C = cyclochexyl

Cp* = 1,2,3,4,5-Pentamethyl-cyclopentadiene

DB = dibenzo

DC = dicyclohexyl

DC18C6-A = cis-syn-cis-dicyclohexyl-[18]crown-6

DCM = Dichloromethane

DME = Dimethoxyethane

DMP = 2,6-dimesitylphenyl

Dppm = 1,1bis(diphe nylphosphino)methane

EDX = energy dispersive X-ray spectroscopy

ELF = electron localization function

ELI = electron localization index

EO5 = pentaethylene glycol

EO6 = hexaethylene glycol

EO7 = heptaethylene glycol

Et = ethyl

EtOH = Ethanol

hfa = hexafluoroacetylacetonate

Me = Methyl

MP2 = Møller–Plesset perturbation theory (2^{nd} order)

NBO = Natural Bond Orbital

NHC = N-heterocyclic Carbene

NPA = Natural Population Analysis

Oda = Oxydiacetate anion

OTf = O_3SCF_3, trifluoromethane sulfonate (triflate)

PEG = poly(ethylene) glycol

Ph = Phenyl

PQTEG = 2-(2-(2-hydroxyethoxy)ethoxy)ethyl 8-propoxyquinoline-2-carboxylate

scXRD = single crystal X-ray diffraction

Tf = O_2SCF_3, trifluoromethanesulfonyl (triflyl)

TFA = O_2CCF_3, trifluoroacetate

XANES = X-ray absorption near edge spectroscopy

6. Acknowledgements

CLBM thanks all of the graduate students, undergraduate students and collaborators who have contributed to our work in this area and to the funding agencies (primarily the Natural Sciences and Engineering Council (NSERC) of Canada, the Canadian Foundation for Innovation (CFI), and the Province of Ontario) who have provided financial support for this work. CLBM also acknowledges Dr. W. Levason and an untimely hard-drive failure for initiating this review.

7. References

1. C. J. Pedersen, *Journal of the American Chemical Society*, 1967, **89**, 7017-7036.
2. C. J. Pedersen, *J. Am. Chem. Soc.*, 1967, **89**, 2495-2496.
3. T. P. Hanusa, in *Coordination Chemistry of the s, p, and f Metals*, Elsevier, Amsterdam, 2003, vol. 3, pp. 1-92.
4. J. L. Dye, M. Y. Redko, R. H. Huang and J. E. Jackson, in *Advances in Inorganic Chemistry: Including Bioinorganic Studies, Vol 59: Template Effects and Molecular Organization*, eds. R. VanEldik and K. BowmanJames, 2007, vol. 59, pp. 205-231.
5. P. C. Junk, *New Journal of Chemistry*, 2008, **32**, 762-773.
6. A. Harada, A. Hashidzume, H. Yamaguchi and Y. Takashima, *Chemical Reviews*, 2009, **109**, 5974-6023.
7. R. A. Potyrailo, *Angewandte Chemie-International Edition*, 2006, **45**, 702-723.
8. G. Aragay, J. Pons and A. Merkoci, *Chemical Reviews*, 2011, **111**, 3433-3458.
9. F. A. Christy and P. S. Shrivastav, *Critical Reviews in Analytical Chemistry*, 2011, **41**, 236-269.
10. R. M. Kakhki, *Journal of Inclusion Phenomena and Macrocyclic Chemistry*, 2013, **75**, 11-22.
11. T. R. Cook, Y. R. Zheng and P. J. Stang, *Chemical Reviews*, 2013, **113**, 734-777.
12. G. W. Gokel and I. A. Carasel, *Chemical Society Reviews*, 2007, **36**, 378-389.
13. D. A. Uhlenheuer, K. Petkau and L. Brunsveld, *Chemical Society Reviews*, 2010, **39**, 2817-2826.
14. M. Kralj, L. Tusek-Bozic and L. Frkanec, *Chemmedchem*, 2008, **3**, 1478-1492.
15. A. A. Elbashir and H. Y. Aboul-Enein, *Current Pharmaceutical Analysis*, 2010, **6**, 101-113.
16. N. Giri, M. G. Del Pópolo, G. Melaugh, R. L. Greenaway, K. Rätzke, T. Koschine, L. Pison, M. F. C. Gomes, A. I. Cooper and S. L. James, *Nature*, 2015, **527**, 216-220.
17. F. H. Allen, *Acta Crystallographica, Section B: Structural Crystallography and Crystal Chemistry*, 2002, **58**, 380-388.
18. G. M. Sheldrick, *Acta Crystallographica Section A*, 2008, **64**, 112-122.
19. J. W. Steed, *Coordination Chemistry Reviews*, 2001, **215**, 171-221.
20. F. Arnaud-Neu, R. Delgado and S. Chaves, *Pure and Applied Chemistry*, 2003, **75**, 71-102.
21. R. Shannon, *Acta Crystallographica Section A*, 1976, **32**, 751-767.

22. B. Cordero, V. Gomez, A. E. Platero-Prats, M. Reves, J. Echeverria, E. Cremades, F. Barragan and S. Alvarez, *Dalton Transactions*, 2008, 2832-2838.
23. C. L. B. Macdonald, B. D. Ellis and A. Swidan, in *Encyclopedia of Inorganic and Bioinorganic Chemistry*, John Wiley & Sons, Ltd, 2012.
24. V. S. V. S. N. Swamy, S. Pal, S. Khan and S. S. Sen, *Dalton Transactions*, 2015, **44**, 12903-12923.
25. G. Parkin, *Journal of Chemical Education*, 2006, **83**, 791-799.
26. C. G. Andrews and C. L. B. Macdonald, *Angewandte Chemie International Edition*, 2005, **44**, 7453-7456.
27. C. L. B. Macdonald, B. D. Ellis and A. a. Swidan, in *Encyclopedia of Inorganic and Bioinorganic Chemistry*, John Wiley & Sons, Ltd, 2011.
28. H. Haddadi, N. Alizadeh, M. Shamsipur, Z. Asfari, V. Lippolis and C. Bazzicalupi, *Inorganic Chemistry*, 2010, **49**, 6874-6882.
29. G. Frenking, R. Tonner, S. Klein, N. Takagi, T. Shimizu, A. Krapp, K. K. Pandey and P. Parameswaran, *Chemical Society Reviews*, 2014, **43**, 5106-5139, and references therein.
30. J. M. Christensen and J. Kristiansen, *Handbook of Metals in Clinical and Analytical Chemistry*, Marcel Dekker, New York, 1994.
31. C. C. Stoumpos, C. D. Malliakas and M. G. Kanatzidis, *Inorganic Chemistry*, 2013, **52**, 9019-9038.
32. R. D. Rogers and A. H. Bond, *Inorganica Chimica Acta*, 1992, **192**, 163-171.
33. R. D. Rogers, A. H. Bond and D. M. Roden, *Inorganic Chemistry*, 1996, **35**, 6964-6973.
34. A. Bashall, M. McPartlin, B. P. Murphy, D. E. Fenton, S. J. Kitchen and P. A. Tasker, *Journal of the Chemical Society, Dalton Transactions*, 1990, 505-509.
35. H. Von Arnim, K. Dehnicke, K. Maczek and D. Fenske, *Zeitschrift für anorganische und allgemeine Chemie*, 1993, **619**, 1704-1712.
36. S. Ulrich, E. Buhler and J. M. Lehn, *New Journal of Chemistry*, 2009, **33**, 271-292.
37. R. D. Hancock, M. Salim Shaikjee, S. M. Dobson and J. C. A. Boeyens, *Inorganica Chimica Acta*, 1988, **154**, 229-238.
38. A. N. Chekhlov, *Russ J Coord Chem*, 2008, **34**, 344-349.
39. A. N. Chekhlov, *Coordination Compounds - Crystal Structure of Bis((1,2-bis(2-(o-hydroxyphenoxy)ethoxy)ethane)(perchlorato-O,O') lead(II))Bis(hydroxide)*, Road Town, 2004.
40. A. N. Chekhlov, *J Struct Chem*, 2006, **47**, 352-361.
41. A. N. Chekhlov, *Russ. J. Inorg. Chem.*, 2006, **51**, 235-240.
42. A. N. Chekhlov, *Russ J Coord Chem*, 2006, **32**, 552-558.
43. A. N. Chekhlov, *Russ J Gen Chem*, 2009, **79**, 1608-1612.
44. A. N. Chekhlov, *Russ. J. Inorg. Chem.*, 2009, **54**, 1981-1986.
45. N. K. Noel, S. D. Stranks, A. Abate, C. Wehrenfennig, S. Guarnera, A.-A. Haghighirad, A. Sadhanala, G. E. Eperon, S. K. Pathak, M. B. Johnston, A. Petrozza, L. M. Herz and H. J. Snaith, *Energy & Environmental Science*, 2014, **7**, 3061-3068.
46. in *The Economist*, The Economist, London, UK, 2015, pp. 71-72.
47. M. E. Lines and A. M. Glass, *Principles and applications of ferroelectrics and related materials*, Clarendon press Oxford, 2001.
48. H.-Y. Ye, Y. Zhang, D.-W. Fu and R.-G. Xiong, *Angewandte Chemie International Edition*, 2014, **53**, 6724-6729.
49. P. Farina, T. Latter, W. Levason and G. Reid, *Dalton Transactions*, 2013, **42**, 4714-4724.
50. G. Malandrino, R. Lo Nigro, P. Rossi, P. Dapporto and I. L. Fragalà, *Inorganica Chimica Acta*, 2004, **357**, 3927-3933.
51. M. A. Chistyakov, E. P. Simonenko, V. G. Sevast'yanov and N. T. Kuznetsov, *Russ J Coord Chem*, 2006, **32**, 693-700.

52. V. G. Sevast'yanov, M. A. Chistyakov, E. P. Simonenko, G. K. Fukin and N. T. Kuznetsov, *Russ J Coord Chem*, 2008, **34**, 157-166.
53. T. M. Polyanskaya, M. A. Chistyakov, E. P. Simonenko, V. G. Sevast'anov and N. T. Kuznetsov, *Inorganica Chimica Acta*, 2009, **362**, 5133-5138.
54. G. Malandrino, R. L. Nigro, P. Rossi, P. Dapport and I. L. Fragala, Electrochemical Society, 2005.
55. M. L. Hitchman and K. F. Jensen, *Chemical Vapor Deposition: Principles and Applications*, Academic Press, 1993.
56. W. J. Evans, D. B. Rego and J. W. Ziller, *Polyhedron*, 2006, **25**, 2691-2697.
57. F. Marandi and H. K. Fun, *Zeitschrift Fur Anorganische Und Allgemeine Chemie*, 2008, **634**, 1123-1126.
58. M. J. Manos, E. E. Moushi, G. S. Papaefstathiou and A. J. Tasiopoulos, *Crystal Growth & Design*, 2012, **12**, 5471-5480.
59. T. M. Reineke, M. Eddaoudi, M. Fehr, D. Kelley and O. M. Yaghi, *Journal of the American Chemical Society*, 1999, **121**, 1651-1657.
60. S. Horike and S. Kitagawa, in *Metal-Organic Frameworks*, Wiley-VCH Verlag GmbH & Co. KGaA, 2011, pp. 1-21.
61. Y.-M. Sun, F.-Y. Dong, J.-M. Dou, X.-K. Gao, D.-C. Li and D.-Q. Wang, *Acta Crystallographica Section E*, 2005, **61**, m1787-m1788.
62. L.-Q. Kong, J.-M. Dou, C.-J. Li, D.-C. Li and D.-Q. Wang, *Acta Crystallographica Section E*, 2006, **62**, m1030-m1032.
63. M. Wolff and C. Feldmann, *Zeitschrift für anorganische und allgemeine Chemie*, 2010, **636**, 1787-1791.
64. F. Rieger and A. V. Mudring, *Zeitschrift Fur Anorganische Und Allgemeine Chemie*, 2008, **634**, 2989-2993.
65. I.-H. Park, K.-M. Park and S. S. Lee, *Dalton Transactions*, 2010, **39**, 9696-9704.
66. R. M. Izatt, K. Pawlak, J. S. Bradshaw and R. L. Bruening, *Chemical Reviews*, 1995, **95**, 2529-2586.
67. B. P. Lanphear, D. A. Burgoon, S. W. Rust, S. Eberly and W. Galke, *Environmental Research*, 1998, **76**, 120-130.
68. D. Esteban-Gómez, C. Platas-Iglesias, F. Avecilla, A. de Blas and T. Rodríguez-Blas, *European Journal of Inorganic Chemistry*, 2007, **2007**, 1635-1643.
69. R. Ferreirós-Martínez, D. Esteban-Gómez, É. Tóth, A. de Blas, C. Platas-Iglesias and T. Rodríguez-Blas, *Inorganic Chemistry*, 2011, **50**, 3772-3784.
70. D. Esteban-Gómez, T. Enríquez-Pérez, R. Ferreirós-Martínez, M. Mato-Iglesias, C. Platas-Iglesias, A. de Blas and T. Rodríguez-Blas, *European Journal of Inorganic Chemistry*, 2010, **2010**, 5027-5034.
71. J. L. Atwood, H. Elgamal, G. H. Robinson, S. G. Bott, J. A. Weeks and W. E. Hunter, *Journal of Inclusion Phenomena*, 1984, **2**, 367-376.
72. J. A. J. Pardoe and A. J. Downs, *Chemical Reviews*, 2007, **107**, 2-45.
73. S. Dagorne and S. Bellemin-Laponnaz, in *The Group 13 Metals Aluminium, Gallium, Indium and Thallium. Chemical Patterns and Peculiarities*, eds. S. Aldridge and A. J. Downs, John Wiley and Sons, Chichester, UK, 2011, pp. 654-700.
74. C. Platas-Iglesias, D. Esteban-Gómez, T. Enríquez-Pérez, F. Avecilla, A. de Blas and T. Rodríguez-Blas, *Inorganic Chemistry*, 2005, **44**, 2224-2233.
75. D. Esteban-Gómez, C. Platas-Iglesias, T. Enríquez-Pérez, F. Avecilla, A. de Blas and T. Rodríguez-Blas, *Inorganic Chemistry*, 2006, **45**, 5407-5416.
76. D. Esteban-Gómez, R. Ferreirós, S. Fernández-Martínez, F. Avecilla, C. Platas-Iglesias, A. de Blas and T. Rodríguez-Blas, *Inorganic Chemistry*, 2005, **44**, 5428-5436.

77. A. I. Vedernikov, E. N. Ushakov, L. G. Kuz'mina, A. V. Churakov, Y. A. Strelenko, M. Wörner, A. M. Braun, J. A. K. Howard, M. V. Alfimov and S. P. Gromov, *Journal of Physical Organic Chemistry*, 2010, **23**, 195-206.
78. J. P. Dix and F. Vögtle, *Angewandte Chemie International Edition in English*, 1978, **17**, 857-859.
79. A. P. de Silva, D. B. Fox, A. J. M. Huxley and T. S. Moody, *Coordination Chemistry Reviews*, 2000, **205**, 41-57.
80. K. Mariappan, M. Alaparthi, M. Hoffman, M. A. Rama, V. Balasubramanian, D. M. John and A. G. Sykes, *Dalton Transactions*, 2015, **44**, 11774-11787.
81. M. Kadarkaraisamy and A. G. Sykes, *Inorganic Chemistry*, 2006, **45**, 779-786.
82. M. Kadarkaraisamy, G. Caple, A. R. Gorden, M. A. Squire and A. G. Sykes, *Inorganic Chemistry*, 2008, **47**, 11644-11655.
83. H. J. Kim, S. H. Kim, J. H. Kim, L. N. Anh, J. H. Lee, C.-H. Lee and J. S. Kim, *Tetrahedron Letters*, 2009, **50**, 2782-2786.
84. S. Park, S. Y. Lee, K.-M. Park and S. S. Lee, *Accounts of Chemical Research*, 2012, **45**, 391-403.
85. R. E. Wolf, J. R. Hartman, J. M. E. Storey, B. M. Foxman and S. R. Cooper, *Journal of the American Chemical Society*, 1987, **109**, 4328-4335.
86. H. Ryu, K.-M. Park, M. Ikeda, Y. Habata and S. S. Lee, *Inorganic Chemistry*, 2014, **53**, 4029-4038.
87. D. Braga, M. Gandolfi, M. Lusi, M. Polito, K. Rubini and F. Grepioni, *Crystal Growth & Design*, 2007, **7**, 919-924.
88. Y. Ma, T. Marszalek, Z. Yuan, R. Stangenberg, W. Pisula, L. Chen and K. Müllen, *Chemistry – An Asian Journal*, 2015, **10**, 139-143.
89. S. Ilhan, *Journal of Chemical Research*, 2009, **2009**, 766-769.
90. S. Ilhan and H. Temel, *Transition Met Chem*, 2007, **32**, 1039-1046.
91. S. Ilhan, H. Temel, R. Ziyadanogullari and M. Sekerci, *Transition Met Chem*, 2007, **32**, 584-590.
92. S. İlhan, *Russ J Coord Chem*, 2009, **35**, 347-351.
93. S. İlhan and H. Temel, *Journal of Coordination Chemistry*, 2009, **62**, 456-464.
94. S. Ilhan, H. Temel and S. Pasa, *Chinese Chemical Letters*, 2009, **20**, 339-343.
95. S. İlhan, *Russ. J. Inorg. Chem.*, 2010, **55**, 583-593.
96. S. Ilhan and H. Temel, *Journal of Chemical Research*, 2010, **34**, 304-306.
97. S. Ilhan, H. Temel, S. Paşa and İ. Teğin, *Russ. J. Inorg. Chem.*, 2010, **55**, 1402-1409.
98. S. Castro-Juiz, A. Fernández, M. López-Torres, D. Vázquez-García, A. J. Suárez, J. M. Vila and J. J. Fernández, *Organometallics*, 2009, **28**, 6657-6665.
99. Ş. Ertul, A. D. Bedük, M. Bayrakci and E. Güler, *Chem. Pap.*, 2008, **62**, 589-595.
100. M. Bayrakcı and Ş. Ertul, *Russ J Org Chem*, 2008, **44**, 1384-1388.
101. J.-C. Aguilar, S. Bernès, P. Gómez-Tagle, R. Bartsch and J. de Gyves, *J Chem Crystallogr*, 2006, **36**, 473-479.
102. P. K. Sazonov, M. S. Grigor'ev, M. M. Shtern, Y. F. Oprunenko, I. G. Tananaev and I. P. Beletskaya, *Russ J Coord Chem*, 2009, **35**, 835-843.
103. P. K. Sazonov, L. K. Minacheva, A. V. Churakov, V. S. Sergienko, G. A. Artamkina, Y. F. Oprunenko and I. P. Beletskaya, *Dalton Transactions*, 2009, 843-850.
104. M. López-Deber, R. Bastida, M. d. C. Fernández-Fernández, A. Macías, A. Rodríguez and L. Valencia, *Zeitschrift für anorganische und allgemeine Chemie*, 2005, **631**, 2033-2040.
105. A. Freiría, R. Bastida, L. Valencia, A. Macías, C. Lodeiro and H. Adams, *Inorganica Chimica Acta*, 2006, **359**, 2383-2394.
106. M. M. Alam, *2011*, 2011, **35**, 5.
107. O. A. Fedorova, A. V. Koshkin, S. P. Gromov, Y. P. Strokach, T. M. Valova, M. V. Alfimov, A. V. Feofanov, I. S. Alaverdian, V. A. Lokshin and A. Samat, *Journal of Physical Organic Chemistry*, 2005, **18**, 504-512.

108. C.-C. Su, *Journal of Molecular Structure*, 2008, **892**, 231-238.
109. A. Yoshida, Y. Nakagawa, K. Uehara, S. Hikichi and N. Mizuno, *Angewandte Chemie International Edition*, 2009, **48**, 7055-7058.
110. M. S. Holt, W. L. Wilson and J. H. Nelson, *Chemical Reviews*, 1989, **89**, 11-49.
111. M. Jiménez-Tenorio, M. D. Palacios, M. C. Puerta and P. Valerga, *Organometallics*, 2004, **23**, 504-510.
112. B. Therrien, T.-T. Thai, J. Freudenreich, G. Süss-Fink, S. S. Shapovalov, A. A. Pasynskii and L. Plasseraud, *Journal of Organometallic Chemistry*, 2010, **695**, 409-414.
113. S. S. Shapovalov, A. A. Pasynskii, Y. V. Torubaev, I. V. Skabitskii, M. Scheer and M. Bodensteiner, *Russ J Coord Chem*, 2014, **40**, 131-137.
114. M. G. Kanatzidis, *Chemistry of Materials*, 1990, **2**, 353-363.
115. M. Wolff, T. Harmening, R. Pöttgen and C. Feldmann, *Inorganic Chemistry*, 2009, **48**, 3153-3156.
116. R. H. Herber and A. E. Smelkinson, *Inorganic Chemistry*, 1978, **17**, 1023-1029.
117. M. G. B. Drew and D. G. Nicholson, *Journal of the Chemical Society, Dalton Transactions*, 1986, 1543-1549.
118. R. Bandyopadhyay, B. F. T. Cooper, A. J. Rossini, R. W. Schurko and C. L. B. Macdonald, *Journal of Organometallic Chemistry*, 2010, **695**, 1012-1018.
119. C. L. B. Macdonald, R. Bandyopadhyay, B. F. T. Cooper, W. W. Friedl, A. J. Rossini, R. W. Schurko, S. H. Eichhorn and R. H. Herber, *Journal of the American Chemical Society*, 2012, **134**, 4332-4345.
120. S. Shaik, D. Danovich, B. Silvi, D. L. Lauvergnat and P. C. Hiberty, *Chemistry-a European Journal*, 2005, **11**, 6358-6371.
121. J. C. Avery, M. A. Hanson, R. H. Herber, K. J. Bladek, P. A. Rupar, I. Nowik, Y. Huang and K. M. Baines, *Inorganic Chemistry*, 2012, **51**, 7306-7316.
122. C. Beattie, P. Farina, W. Levason and G. Reid, *Dalton Transactions*, 2013, **42**, 15183-15190.
123. A. C. T. Kuate, G. Reeske, M. Schuermann, B. Costisella and K. Jurkschat, *Organometallics*, 2008, **27**, 5577-5587.
124. L. Wang, S.-C. Rosca, V. Poirier, S. Sinbandhit, V. Dorcet, T. Roisnel, J.-F. Carpentier and Y. Sarazin, *Dalton Transactions*, 2014, **43**, 4268-4286.
125. Y. Sarazin, D. L. Hughes, N. Kaltsoyannis, J. A. Wright and M. Bochmann, *Journal of the American Chemical Society*, 2007, **129**, 881-894.
126. S. G. Bott, H. Prinz, A. Alvanipour and J. L. Atwood, *Journal of Coordination Chemistry*, 1987, **16**, 303-309.
127. V. K. Belskii, B. M. Bulychev, N. R. Streltsova, P. A. Storozhenko and L. V. Ivakina, *Doklady Akademii Nauk Sssr*, 1988, **303**, 1137-1140.
128. A. C. Tagne Kuate, M. Schürmann, D. Schollmeyer, W. Hiller and K. Jurkschat, *Chemistry – A European Journal*, 2010, **16**, 8140-8146.
129. A. C. T. Kuate, L. Iovkova, W. Hiller, M. Schuermann and K. Jurkschat, *Organometallics*, 2010, **29**, 5456-5471.
130. V. Arens, C. Dietz, D. Schollmeyer and K. Jurkschat, *Organometallics*, 2013, **32**, 2775-2786.
131. V. A. Uchtman and R. P. Oertel, *Journal of the American Chemical Society*, 1973, **95**, 1802-1811.
132. P. J. Sheffield, U. Derewenda, J. Taylor, T. J. Parsons and Z. S. Derewenda, *Acta Crystallographica Section D*, 1999, **55**, 356-359.
133. C. Di Nicola, A. Galindo, J. V. Hanna, F. Marchetti, C. Pettinari, R. Pettinari, E. Rivarola, B. W. Skelton and A. H. White, *Inorganic Chemistry*, 2005, **44**, 3094-3102.
134. P. A. Rupar, V. N. Staroverov and K. M. Baines, *Science*, 2008, **322**, 1360-1363.
135. H. V. R. Dias and Z. Wang, *Journal of the American Chemical Society*, 1997, **119**, 4650-4655.
136. M. Stender, A. D. Phillips and P. P. Power, *Inorganic Chemistry*, 2001, **40**, 5314-5315.

137. F. Cheng, A. L. Hector, W. Levason, G. Reid, M. Webster and W. J. Zhang, *Angewandte Chemie-International Edition*, 2009, **48**, 5152-5154.
138. P. A. Rupar, R. Bandyopadhyay, B. F. T. Cooper, M. R. Stinchcombe, P. J. Ragogna, C. L. B. Macdonald and K. M. Baines, *Angewandte Chemie-International Edition*, 2009, **48**, 5155-5158.
139. F. Scholz, H. Kahlert, U. Hasse, A. Albrecht, A. C. T. Kuate and K. Jurkschat, *Electrochemistry Communications*, 2010, **12**, 955-957.
140. A. C. T. Kuate, M. Schuermann, D. Schollmeyer, W. Hiller and K. Jurkschat, *Chemistry-a European Journal*, 2010, **16**, 8140-8146.
141. A. L. Hector, W. Levason, G. Reid, M. Webster and W. J. Zhang, *Dalton Transactions*, 2011, **40**, 694-700.
142. F. Cheng, A. L. Hector, W. Levason, G. Reid, M. Webster and W. Zhang, *Chemical Communications*, 2008, 5508-5510.
143. W. Levason, S. D. Orchard and G. Reid, *Coordination Chemistry Reviews*, 2002, **225**, 159-199.
144. W. Levason, G. Reid and W. Zhang, *Dalton Transactions*, 2011, **40**, 8491-8506.
145. W. Levason, G. Reid and W. Zhang, *Coordination Chemistry Reviews*, 2011, **255**, 1319-1341.
146. R. Bandyopadhyay, J. H. Nguyen, A. Swidan and C. L. B. Macdonald, *Angewandte Chemie-International Edition*, 2013, **52**, 3469-3472.
147. S. Aldridge and A. J. Downs, eds., *The Group 13 Metals Aluminium, Gallium, Indium and Thallium. Chemical Patterns and Peculiarities*, John Wiley & Sons, Chichester, UK, 2011.
148. N. Ajellal, J.-F. Carpentier, C. Guillaume, S. M. Guillaume, M. Helou, V. Poirier, Y. Sarazin and A. Trifonov, *Dalton Trans.*, 2010, **39**, 8363-8376.
149. P. Jutzi, A. Mix, B. Rummel, W. W. Schoeller, B. Neumann and H.-G. Stammler, *Science*, 2004, **305**, 849-851.
150. K. Leszczynska, A. Mix, R. J. F. Berger, B. Rummel, B. Neumann, H. G. Stammler and P. Jutzi, *Angewandte Chemie-International Edition*, 2011, **50**, 6843-6846.
151. C. Jones and A. Stasch, in *The Group 13 Metals Aluminium, Gallium, Indium and Thallium. Chemical Patterns and Peculiarities*, eds. S. Aldridge and A. J. Downs, John Wiley and Sons, Chichester, UK, 2011, pp. 285-341.
152. P. Jutzi and N. Burford, *Chemical Reviews*, 1999, **99**, 969-990.
153. C. Jones and A. Stasch, in *The Group 13 Metals Aluminium, Gallium, Indium and Thallium: Chemical Patterns and Peculiarities*, John Wiley & Sons, Ltd, 2011, pp. 285-341.
154. A.-V. Mudring and F. Rieger, *Inorganic Chemistry*, 2005, **44**, 6240-6243.
155. F. Liu, *Applied Organometallic Chemistry*, 2003, **17**, 737-738.
156. N. S. Fender, S. S. Finegan, D. Miller, M. Mitchell, I. A. Kahwa and F. R. Fronczek, *Inorganic Chemistry*, 1994, **33**, 4002-4008.
157. F. Rieger and A. V. Mudring, *Inorganic Chemistry*, 2005, **44**, 9340-9346.
158. I. Brown, *Acta Crystallographica Section B*, 1988, **44**, 545-553.
159. M. L. Gill, S. A. Strobel and J. P. Loria, *Journal of the American Chemical Society*, 2005, **127**, 16723-16732.
160. E. D. Roper, V. S. Talanov, R. J. Butcher and G. G. Talanova, *Supramolecular Chemistry*, 2008, **20**, 217-229.
161. E. D. Roper, V. S. Talanov, M. G. Gorbunova, R. A. Bartsch and G. G. Talanova, *Analytical Chemistry*, 2007, **79**, 1983-1989.
162. S. Spirk, F. Belaj, M. Nieger, H. Köfeler, G. N. Rechberger and R. Pietschnig, *Chemistry – A European Journal*, 2009, **15**, 9521-9529.
163. H. Vonarnim and K. Dehnicke, *Zeitschrift Fur Naturforschung Section B-a Journal of Chemical Sciences*, 1993, **48**, 1331-1340.
164. J. Massaux and J. F. Desreux, *Journal of the American Chemical Society*, 1982, **104**, 2967-2972.

165. M. L. C. R. H. C. Jones, *Main Group Metal Chemistry*, 2011, **24**, 819-820.
166. K. Kobiro, M. Takahashi, Y. Odaira, Y. Kawasaki, Y. Kai and N. Kasai, *Journal of the Chemical Society, Dalton Transactions*, 1986, 2613-2615.
167. K. Kobiro, S. Takada, Y. Odaira and Y. Kawasaki, *Journal of the Chemical Society, Dalton Transactions*, 1986, 1767-1769.
168. D. L. Hughes and M. R. Truter, *Acta Crystallographica Section B*, 1983, **39**, 329-336.
169. J. A. J. Pardoe and A. J. Downs, *Chemical Reviews*, 2007, **107**, 2-45.
170. S. P. Green, C. Jones and A. Stasch, *Chemical Communications*, 2008, 6285-6287.
171. R. J. Baker and C. Jones, *Dalton Transactions*, 2005, 1341-1348.
172. C. L. B. Macdonald, A. M. Corrente, C. G. Andrews, A. Taylor and B. D. Ellis, *Chemical Communications*, 2004, 250-251.
173. B. F. T. Cooper and C. L. B. Macdonald, *Journal of Organometallic Chemistry*, 2008, **693**, 1707-1711.
174. O. T. Beachley, Jr., R. Blom, M. R. Churchill, K. Faegri, Jr., J. C. Fettinger, J. C. Pazik and L. Victoriano, *Organometallics*, 1989, **8**, 346-356.
175. B. F. T. Cooper and C. L. B. Macdonald, *New Journal of Chemistry*, 2010, **34**, 1551-1555.
176. B. F. T. Cooper, H. Hamaed, W. W. Friedl, M. R. Stinchcombe, R. W. Schurko and C. L. B. Macdonald, *Chemistry – A European Journal*, 2011, **17**, 6148-6161.
177. B. F. T. Cooper and C. L. B. Macdonald, in *The Group 13 Metals Aluminium, Gallium, Indium and Thallium. Chemical Patterns and Peculiarities*, eds. S. Aldridge and A. J. Downs, John Wiley and Sons, Chichester, UK, 2011, pp. 342-401.
178. H. Hamaed, K. E. Johnston, B. F. T. Cooper, V. V. Terskikh, E. Ye, C. L. B. Macdonald, D. C. Arnold and R. W. Schurko, *Chemical Science*, 2014, **5**, 982-995.
179. B. F. T. Cooper and C. L. B. Macdonald, *Main Group Chemistry*, 2010, **9**, 141-152.
180. A. Higelin, C. Haber, S. Meier and I. Krossing, *Dalton Transactions*, 2012, **41**, 12011-12015.
181. I. Krossing and I. Raabe, *Angewandte Chemie-International Edition*, 2004, **43**, 2066-2090.
182. I. Krossing and A. Reisinger, *Coordination Chemistry Reviews*, 2006, **250**, 2721-2744.
183. B. F. T. Cooper and C. L. B. Macdonald, *Acta Crystallographica Section E*, 2011, **67**, m233-m234.
184. B. F. T. Cooper, C. G. Andrews and C. L. B. Macdonald, *Journal of Organometallic Chemistry*, 2007, **692**, 2843-2848.
185. G. R. Willey, D. R. Aris and W. Errington, *Inorganica Chimica Acta*, 2000, **300–302**, 1004-1013.
186. J. M. Slattery, A. Higelin, T. Bayer and I. Krossing, *Angewandte Chemie-International Edition*, 2010, **49**, 3228-3231.
187. J. L. Bourque, P. D. Boyle and K. M. Baines, *Chemistry – A European Journal*, 2015, **21**, 9790-9796.
188. G. H. Robinson, W. E. Hunter, S. G. Bott and J. L. Atwood, *Journal of Organometallic Chemistry*, 1987, **326**, 9-16.
189. B. Lee, W. T. Pennington and G. H. Robinson, *Organometallics*, 1990, **9**, 1709-1711.
190. B. Jisha, M. R. Resmi, R. J. Maya and R. L. Varma, *Tetrahedron Letters*, 2013, **54**, 4232-4236.
191. S. G. Bott, H. Elgamal and J. L. Atwood, *Journal of the American Chemical Society*, 1985, **107**, 1796-1797.